CONFIDENTIAL

Copy No. 346
RM No. A8E05

NACA RM No. A8E05

NACA

RESEARCH MEMORANDUM

INVESTIGATION OF WING CHARACTERISTICS AT A MACH NUMBER OF 1.53. II - SWEPT WINGS OF TAPER RATIO 0.5

By Walter G. Vincenti, Milton D. Van Dyke, and Frederick H. Matteson

Ames Aeronautical Laboratory
Moffett Field, Calif.

NATIONAL ADVISORY COMMITTEE FOR AERONAUTICS

WASHINGTON

June 28, 1948

CONFIDENTIAL

NATIONAL ADVISORY COMMITTEE FOR AERONAUTICS

RESEARCH MEMORANDUM

INVESTIGATION OF WING CHARACTERISTICS AT A MACH NUMBER OF 1.53. II - SWEPT WINGS OF TAPER RATIO 0.5

By Walter G. Vincenti, Milton D. Van Dyke, and Frederick H. Matteson

SUMMARY

As the second part of a general study of wing characteristics at supersonic speed, wind-tunnel tests were conducted at a Mach number of 1.53 of seven wings varying in angle of sweep from 60° sweepforward to 60° sweepback. The wings had a uniform isosceles-triangle section 5-percent thick and a common taper ratio of 0.5. The range of sweep angles provided both supersonic and subsonic leading and trailing edges at the test Mach number. Measurements were made of lift, drag, and pitching moment at a Reynolds number of 0.75 million. In the present report, the experimental results are analyzed and compared with characteristics calculated by means of linear theory.

The experimental values of the lift-curve slope were found to agree reasonably with theory over the complete range of sweep angles. Because of secondary differences, however, the experimental variation was not, as theory would predict, completely symmetrical with respect to direction of sweep. The experimental angles of zero lift were significantly higher than the theoretical, probably as a result of the higher-order pressure effects neglected in the linear theory.

With regard to moment-curve slope, the experimental values indicated a variation of aerodynamic-center position with angle of sweep opposite to that predicted by theory, with individual discrepancies up to 17 percent of the mean aerodynamic chord. The measured values of the moment coefficient at zero lift were consistently negative and agreed well with the theoretical calculations.

The experimental minimum drag was almost exactly symmetrical with respect to direction of sweep and had the general character predicted by the linear theory. The measured increase in minimum drag for sweep angles in the vicinity of the Mach cone was, however, less pronounced than theory would predict.

For the wings with a supersonic leading edge, the increase in drag with angle of attack indicated that the rearward rotation of the change in resultant force was approximately equal to the accompanying change in angle. For the swept-back wing with a subsonic leading edge, the rotation of the force vector was less than the change in angle despite the sharp leading edge and presumed absence of leading-edge suction. This result was found to be in accord with the results of two-dimensional subsonic tests of sharp-edged airfoils.

For the wings considered (isosceles-triangle section), the experimental maximum lift-drag ratio was between 6 and $6\frac{1}{2}$ over the complete range of sweep angles.

INTRODUCTION

This is the second of a series of reports covering a study at a Mach number of 1.53 of wings of varying plan form and section. Part I of the series (reference 1) was concerned with changes in section for wings of a single triangular plan form. The present report discusses the effects of variation in angle of sweep for a family of moderately tapered wings.

The family of wings considered here had a uniform taper ratio of 0.5 and an isosceles-triangle section 5-percent thick in the streamwise direction. The angle of sweep of the midchord line varied from 60° sweepforward to 60° sweepback, a range which provided subsonic and supersonic leading and trailing edges for both the swept-forward and swept-back plan forms.[1] The experimental results for these wings are discussed in detail and compared with the calculated results of the linear theory.

---

[1]An element of the wing is described as subsonic or supersonic, depending on whether the normal component of the free-stream velocity is subsonic or supersonic - or, in other words, whether the local angle of sweep is greater or less than the sweep angle of the Mach cone. When the local angle of sweep is equal to that of the Mach cone, the element is described as sonic.

SYMBOLS

Primary Symbols

A	aspect ratio
b	wing span
c	wing chord measured in streamwise direction
$\bar{c}_a$	mean aerodynamic chord $\left(\frac{2}{S}\int_0^{b/2} c^2\, db\right)$
$\bar{c}_g$	mean geometric chord (S/b)
c_r	wing root chord
c_t	wing tip chord
C_D	total drag coefficient
$C_{D_{cc}}$	pressure drag coefficient of cambered surface due to own pressure field
$C_{D_{ca}}$	pressure drag coefficient of cambered surface due to pressure field of flat-plate wing
C_{D_f}	friction drag coefficient
$C_{D_{min}}$	minimum total drag coefficient
C_{D_t}	pressure drag coefficient due to thickness
ΔC_D	rise in drag coefficient above minimum $(C_D - C_{D_{min}})$; replaces the symbol C_{D_i} used for the same quantity in Part I
C_L	lift coefficient
C_{L_a}	lift coefficient of flat-plate wing
$C_{L_{opt}}$	lift coefficient for maximum lift-drag ratio
$\frac{dC_L}{d\alpha}$	lift-curve slope (per radian unless otherwise specified)
ΔC_L	change in lift coefficient from value for minimum drag $(C_L - C_{L_{D_{min}}})$

$\frac{\Delta C_D}{(\Delta C_L)^2}$	drag-rise factor
$\left(\frac{L}{D}\right)_{max}$	maximum lift-drag ratio
C_m	pitching-moment coefficient about centroid of plan-form area with mean aerodynamic chord as reference length
$\frac{dC_m}{dC_L}$	moment-curve slope
k_a	angle ratio $[\alpha_{\Delta L}/(\alpha-\alpha_{D=min})]$
m	ratio of tangent of wing semiapex angle to tangent of Mach angle
M_o	free-stream Mach number
Re	Reynolds number based on mean geometric chord of wing
S	wing plan-form area
S_T	wing area of triangular wing having same leading edge as given swept wing
$\frac{t}{c}$	thickness ratio of streamwise wing section
$\bar{x}$	distance back from leading edge of root chord to aerodynamic center (In applications to component flat-plate wings, each wing is considered as a separate entity with its own leading edge and aerodynamic center.)
x_o	distance back from leading edge of root chord to centroid of plan-form area (Symbol used in application to complete wing only.)
$\frac{y_c}{c}$	camber ratio of streamwise wing section
α	angle of attack
α_a	rearward rotation of force vector on flat-plate wing of same plan form as given complete wing

$\alpha_{\Delta L}$ rearward rotation of the change in resultant force corresponding to the change in lift coefficient ΔC_L

Λ_0 sweep angle of leading edge, degrees

$\Lambda_{\frac{1}{2}}$ sweep angle of midchord line, degrees

Λ_1 sweep angle of trailing edge, degrees

Subscripts

L=0 value at zero lift

D=min value at minimum drag

α=0 value at zero angle of attack

P refers to primary wing (i.e., flat-plate wing of same plan form as given complete wing)

F refers to front-half component wing (i.e., flat-plate wing having same plan form as region ahead of ridge line)

R refers to rear-half component wing (i.e., flat-plate wing having same plan form as region behind ridge line)

EXPERIMENTAL CONSIDERATIONS

The investigation was conducted in the Ames 1- by 3-foot supersonic wind tunnel No. 1. The experimental procedure employed throughout the general study is described in Part I of the present series of reports (reference 1). Except where specifically noted, all details of model construction and support, experimental technique, and reduction and correction of data may be taken as identical with those described in Part I.

Models

A photograph of the present models is presented in figure 1(a); one of the models is shown mounted in the tunnel in figure 1(b). The dimensions of the wing models are given in figure 2; the dimensions of the support body can be found in figure 3 of Part I.

The design of the models and body was such that a model of nonsymmetrical plan form could be tested either as a swept-back or swept-forward wing. The four models used thus provided seven essentially different wings. A summary of the geometrical characteristics of these wings is given in table I at the end of the text.

For all of the wings the airfoil section taken in the streamwise direction was a 5-percent-thick isosceles triangle - that is, a triangle with 5-percent maximum thickness located at midchord. This section, which was chosen primarily for ease of construction, was the same as that of wings SBT-3 and SFT-3 of Part I. The plan forms, including the portion enclosed by the support body, were of taper ratio 0.5 and had a uniform area of 9 square inches. The seven wings of the series included angles of sweep, measured at the midchord line, of 0°, $\pm 30^\circ$, $\pm 43^\circ$, and $\pm 60^\circ$. The aspect ratio for the series was made equal to four times the cosine of the angle of sweep, since a constant aspect ratio did not appear desirable structurally. The sweep angles were chosen to provide wings having both supersonic and subsonic leading edges. The wing of 43° sweepback was designed to have its leading edge coincident with the Mach cone at the test Mach number.

For purposes of consistency with a later report in this series, the unswept wing of the present report is referred to here as wing U-2. The swept models themselves are identified by the letter S together with a numeral 1, 2, or 3 in the order of increasing absolute sweep. A second letter F or B is used to indicate whether a given swept model is being considered as a swept-forward or swept-back wing. The designation SB-3, for example, thus denotes the most highly swept-back wing.

The leading and trailing edges of the models were maintained sharp to less than 0.001-inch radius in the first tests. As with wing SBT-1 of Part I, wing SB-3 was subsequently tested with the leading edge rounded successively to radii of 0.25 and 0.50 percent of the chord.

Corrections and Precision

For reasons discussed in Part I, no correction has been applied to the data for the tare and interference effects of the support body. In other words, the experimental results are, in each case, for the wing-body combination rather than for the wing alone. In order to eliminate the effect of variation in balance-cap interference, the drag data have been reduced, as in the earlier paper,

to a common support-body base pressure equal to the static pressure of the free stream. The angles of attack have been corrected for stream angularity as explained in Part I.

The precision of the present results is the same as that of the results of Part I (p. 13), except with regard to the angle of attack. In the present investigation an additional uncertainty is introduced into this quantity by the effective twist which a swept wing experiences under load. As a result primarily of wing bending, the angle of attack of streamwise sections varied across the span during test, the angle increasing toward the tip with positive lift for a swept-forward wing and decreasing for a swept-back wing. The angles of attack at the root and tip of each swept wing were measured by observation with a telescope during the test. In every case, the measured relative twist was between 5 and 10 percent of the angle of attack at the root. All final results are presented, however, in terms of the angle of attack at the wing root as determined by the method described in reference 1.

THEORETICAL CONSIDERATIONS

General equations for the lift, pitching-moment, and drag curves, as deduced from the assumptions of the linear theory, are given in Part I (reference 1). For five of the seven present wings, existing theory allowed rigorous analytical determination, exclusive of the effects of viscosity, of all terms in these equations. For the most highly swept-back wing, calculation of the terms affected by camber was not tried, and certain minor violations of the boundary conditions had to be introduced in obtaining the remaining terms. For the most highly swept-forward wing, no calculations were attempted. As in Part I, the effects of angle of attack, camber, and thickness were considered separately in determining the pressure distribution - and hence the aerodynamic characteristics - of any given wing. (The detailed calculations were made in each case for an equivalent wing at a Mach number of $\sqrt{2}$ and the characteristics of the actual wing at the test Mach number were then derived by means of the transformation rule described in reference 2.) As an aid in the later discussion of the experimental results, the characteristics of the airfoil section in two-dimensional supersonic flow were also calculated with the available higher-order theories.

Lift and Moment Curves – Linear Theory

The lift and moment curves predicted by the linear theory are traight lines. The slopes $dC_L/d\alpha$ and dC_m/dC_L are determined ompletely by the pressure distribution due to angle of attack – hat is, by the pressure distribution at angle of attack over a lat plate having the same plan form as the given wing. The ıtercepts $\alpha_{L=0}$ and $C_{m_{L=0}}$ depend also on the pressure distribu- on due to camber, which is defined as the distribution of pressure zero angle of attack over an infinitesimally thin surface having e same plan form and camber as the given wing.

The pressure distribution due to angle of attack is obtained considering the flat-plate wing to be divided, as shown in gure 3, into polygonal regions determined by the Mach lines iginating at the corners of the plan form. The pressure field thin these regions can be calculated in many cases by means of xisting analytical results. References applicable to the present wings are indicated for each region by the circled numerals in figure 3. (See references 3, 4, 5, 6, 7, and 8.)

For all the plan forms except those of 60° sweep, the pressure distribution for the entire flat-plate wing could be calculated rigorously by means of the existing solutions noted in the figure. For wing SB-3, the calculation of the pressure field at the tips and near the trailing edge by the method of reference 8 involved minor violations of the boundary conditions, so that the results for this wing must be considered as approximate even within the limits of the linear theory. The degree of approximation should, however, be close. For wing SF-3, the pressure field for a large portion of the wing could not be determined from known solutions, and no analysis was attempted. Over the rear portion of this wing, multiple reflection of the Mach lines takes place in much the same manner as on the swept-forward triangular plan form discussed in Appendix B of Part I. The problem here, however, is complicated by the presence of the subsonic leading edge.

Once the expressions for the pressure distribution due to angle of attack are known, the values of the lift- and moment-curve slopes are found by integration. For the present study, it was necessary to go through the complete analysis for wings SB-2 and SF-2 only. For the wings of lesser sweep, the final equations of Lagerstrom (reference 6) are applicable, although an independent analysis was carried out as a check. For wing SB-3, the equations of Cohen (reference 8) were used directly.

For every case in which results could be obtained for wings of equal forward and backward sweep, the theoretical values of the lift-curve slope for the two cases were found to be identical. This result was noted previously by Lagerstrom (reference 6) for a class of plan forms of limited sweep. This class, which includes wings SB-1 and SF-1 from the present study, is defined by the restrictions that the Mach lines from the leading edge of the root must cross the trailing edge, and those from the leading edge of the tips must intersect each other off the plan form. (A necessary but not sufficient condition for this to occur is that the leading and trailing edges be supersonic.) In the case of wings SB-2 and SF-2, the result is here extended to a pair of wings swept to such an extent that in the swept-back case the leading edge coincides with its own Mach cone. Furthermore, the analysis of Appendix B of Part I strongly suggests that the result also holds true for a triangular plan form the swept edge of which is subsonic. It thus seems likely that the independence principle is more general than the present specific calculations would indicate. Consequently, the lift-curve slope for the most highly swept-forward wing, SF-3, which could not be calculated, has been assumed equal to that for its swept-back counterpart.

The pressure distribution due to camber for all but the wings of 60° sweep can be found by superposition of the pressure distributions due to angle of attack for suitable flat-plate wings. It is only necessary that the flow fields of the component flat surfaces shall when added satisfy the boundary conditions imposed by the complete camber surface. When the ridge line is supersonic, as is the case for all of the present wings except SB-3 and SF-3, this condition is satisfied by the superposition of two component surfaces: (1) a flat plate having the same plan form as the camber surface and placed at an angle of attack of $-2(y_c/c)$, where y_c/c is the camber at the ridge line expressed as a fraction of the local chord; (2) a flat plate having a plan form and position corresponding to the region behind the ridge line and placed at an angle of attack of $4(y_c/c)$. The first component surface, called the primary surface, is identical with the flat plate used in finding the pressure distribution due to angle of attack for the complete wing (fig. 3). The pressure distribution of the second - or rear-half - surface can in each case be found in the same general manner.

The lift and moment for the given complete wing at zero angle of attack are identical with the lift and moment of the camber surface and can be found by integration of the pressure distribution due to camber. For wings with a supersonic ridge line at midchord, the results can be expressed directly in terms of the characteristics

of the component surfaces by the equations

$$C_{L_{\alpha=0}} = -2\left(\frac{y_c}{c}\right)\left[\left(\frac{dC_L}{d\alpha}\right)_P - \left(\frac{dC_L}{d\alpha}\right)_R\right] \tag{1}$$

$$C_{m_{\alpha=0}} = -\frac{2(y_c/c)}{\bar{c}_a}\left[\left(\frac{dC_L}{d\alpha}\right)_P (x_o - \bar{x}_P) + \left(\frac{dC_L}{d\alpha}\right)_R \left(\bar{x}_R + \frac{c_r}{2} - x_o\right)\right] \tag{2}$$

where the subscripts P and R refer to the primary and rear-half surfaces, respectively. In these and succeeding equations, the various lift-curve slopes are evaluated as though each surface were a separate wing. The fact that the partial surfaces have one-half the actual area of the primary surface is taken into account in the derivation of the equations. The distances $\bar{x}$ (see list of symbols for definition) are in each case taken between the leading edge of the component surface and the corresponding aerodynamic center. Values of angle of zero lift and moment at zero lift for the complete wing can be calculated from equations (1) and (2) in conjunction with equations (2) and (4) of Part I. For application to wings of the present isosceles-triangle section, the quantity y_c/c in the present equations may be replaced by the equivalent quantity $t/2c$.

When the ridge line is subsonic, as on wing SB-3 and SF-3, the foregoing method for the treatment of camber fails, since the rear-half surface then induces upwash ahead of the ridge and so violates the boundary conditions for the camber surface in this region. In such cases, the problem is considerably more difficult, and no solution was attempted.

Drag Curve – Linear Theory

Using the notation $\Delta C_D = (C_D - C_{D_{min}})$ and $\Delta C_L = (C_L - C_{L_{D=min}})$, the drag curve of the linear theory can be written in the parabolic form[2]

$$C_D = C_{D_{min}} + \frac{\Delta C_D}{(\Delta C_L)^2}(C_L - C_{L_{D=min}})^2 \tag{3}$$

[2]The symbol ΔC_D is used here in place of the symbol C_{D_i} employed for the same quantity in Part I.

The derivation of this equation was indicated in Part I, page 16, for the case of zero leading-edge suction only. Its form can be shown to be unaltered by the presence of the suction which theory predicts on a subsonic leading edge. The value of the individual terms, however, will be affected.

For any wing with a supersonic leading edge, no leading-edge suction is theoretically possible. The quantities $C_{D_{min}}$ and $C_{L_{D=min}}$ are then given by equations (8) and (10) of Part I as

$$C_{D_{min}} = C_{D_f} + C_{D_t} + C_{D_{cc}} - \frac{1}{4(dC_L/d\alpha)}\left(C_{L_{\alpha=0}} + \frac{dC_{D_{ca}}}{d\alpha}\right)^2 \qquad (4)$$

and

$$C_{L_{D=min}} = \frac{1}{2}\left(C_{L_{\alpha=0}} - \frac{dC_{D_{ca}}}{d\alpha}\right) \qquad (5)$$

The analagous general expressions for wings with a subsonic leading edge were not derived in view of the difficulties which could be foreseen in the numerical evaluation of the terms affected by camber.

The friction drag coefficient C_{D_f} in equation (4) has been disregarded in the drag computations of the present paper. An expression for its estimation is given by equation (5) of Part I.

The drag coefficient due to thickness C_{D_t} is determined for any wing by the pressure distribution at zero angle of attack over an uncambered wing of the same thickness distribution as the given wing (Part I, pp. 13 to 16). The value of C_{D_t} for all of the present wings was calculated by application of the source-sink method of Jones (reference 9). As indicated by von Kármán (reference 10), this component of drag is, for an object of given shape and to the order of approximation of the linear theory, unchanged by reversal of the direction of motion. Thus, for a given model in the present paper, the drag due to thickness is independent of the direction of sweep. It was sufficient, therefore, to perform the details of the swept-wing calculations of C_{D_t} for the swept-back case only. Certain of the wings can also be handled directly by means of the equations and graphs of references 6, 11, and 12.

The term $C_{D_{cc}}$ in equation (4) is the drag of the pressure distribution due to camber acting on the elementary camber surface. (See Part I, p. 15.) As with the previous quantities depending on camber, the value of $C_{D_{cc}}$ for the wings with a supersonic ridge line can be expressed in terms of the characteristics of component flat surfaces. Because of considerations of surface slope, however, care must be taken here to conceive of the component pressures as acting upon the complete camber surface rather than upon the two component surfaces introduced to determine the pressure. This requires the introduction of a third component surface, called the front-half surface, which has a position and plan form corresponding to the region ahead of the ridge line. The term $C_{D_{cc}}$ is then given for the present wings by the equation

$$C_{D_{cc}} = 4\left(\frac{y_c}{c}\right)^2\left[\left(\frac{dC_L}{d\alpha}\right)_F + \left(\frac{dC_L}{d\alpha}\right)_R - \left(\frac{dC_L}{d\alpha}\right)_P\right] \qquad (6)$$

where the new subscript F refers to the front-half surface.

The value of the quantity $dC_{D_{ca}}/d\alpha$ in equations (4) and (5) is found by evaluating the drag of the camber surface when subjected to the pressure field of the flat-plate wing used to determine the effects of angle of attack. Since this latter wing is identical with the primary surface used in the treatment of camber, an equation for this quantity can be written

$$\frac{dC_{D_{ca}}}{d\alpha} = 2\left(\frac{y_c}{c}\right)\left[\left(\frac{dC_L}{d\alpha}\right)_F - \left(\frac{dC_L}{d\alpha}\right)_P\right] \qquad (7)$$

This expression, when combined with equation (1) of the present report, gives for the final term in equation (4)

$$\frac{1}{4(dC_L/d\alpha)}\left(C_{L_{\alpha=0}} + \frac{dC_{D_{ca}}}{d\alpha}\right)^2 = \frac{(y_c/c)^2}{(dC_L/d\alpha)_P}\left[\left(\frac{dC_L}{d\alpha}\right)_F + \left(\frac{dC_L}{d\alpha}\right)_R - 2\left(\frac{dC_L}{d\alpha}\right)_P\right]^2 \qquad (8)$$

and equation (5) becomes

$$C_{L_{D=min}} = \left(\frac{y_c}{c}\right)\left[\left(\frac{dC_L}{d\alpha}\right)_R - \left(\frac{dC_L}{d\alpha}\right)_F\right] \tag{9}$$

Equations (6) through (9), together with equations (1) and (2), apply only to uniformly tapered wings having the present type of mean camber surface with ridge line at midchord. As with equations (1) and (2), it is also necessary that the ridge line be supersonic. Equations (6) through (9) are, in addition, subject to the restriction of equations (4) and (5) that the leading edge be supersonic so that no leading-edge suction need be considered.

The foregoing equations were used to calculate the minimum drag characteristics (excluding friction drag) for all of the wings to which they are applicable. For wing SB-3 and SF-3, the method does not apply, since both the ridge line and leading edge are subsonic. As before, no solution for these wings was attempted.

Since the lift curve of the linear theory is a straight line, the drag-rise factor in equation (3) can be expressed in the form

$$\frac{\Delta C_D}{(\Delta C_L)^2} = \frac{\Delta C_D/\Delta C_L}{(dC_L/d\alpha)(\alpha-\alpha_{D=min})} \simeq \frac{\alpha_{\Delta L}/(\alpha-\alpha_{D=min})}{dC_L/d\alpha} \tag{10}$$

Here $\alpha_{\Delta L}$ is the rearward rotation of the change in resultant force corresponding to the change in lift ΔC_L. The angle ratio $\alpha_{\Delta L}/(\alpha-\alpha_{D=min})$ defines this inclination as a fraction of the accompanying change in angle of attack. Introducing the definition

$$k_a \equiv \frac{\alpha_{\Delta L}}{\alpha-\alpha_{D=min}} \simeq \frac{\Delta C_D/\Delta C_L}{\alpha-\alpha_{D=min}} \tag{11}$$

equation (10) is finally written

$$\frac{\Delta C_D}{(\Delta C_L)^2} = \frac{k_a}{dC_L/d\alpha} \tag{12}$$

In the linear theory, the value of k_a, like that of the lift-curve slope $dC_L/d\alpha$, is determined completely by the pressure distribution due to angle of attack. It can be expressed for plan forms with either a subsonic or supersonic leading edge by the relation

$$k_a = \frac{\alpha_a}{\alpha} \tag{13}$$

That is, k_a is given directly by the rearward rotation α_a of the force vector on the elementary flat-plate wing expressed as a fraction of the angle of attack.[3]

As discussed in Part I (p. 17), the theoretical value of k_a in equation (12) is unity for a wing with a supersonic leading edge. For a wing with a subsonic leading edge, however, linear

---

[3]Equations (12) and (13) were given in Part I (p. 16) as applying only to uncambered wings. It can be shown that they are unaltered by the presence of camber. This follows from consideration, when both camber and leading-edge suction are present, of the nature of the various terms in the general drag equation on page 15 of Part I. When the terms in this equation are expanded with C_L as the independent variable, the drag-rise factor, which is identically equal to the coefficient of C_L^2 in the resulting quadratic equation, is found to depend upon the characteristics of the flat-plate wing only. This result was previously indicated in equation (9) of Part I for the special case of zero leading-edge suction.

theory indicates a value less than unity as a result of leading-edge suction. For a swept-back wing of the present general type, the amount of theoretical leading-edge suction at a given Mach number equals that for a swept-back triangular wing having the same leading edge. This is true as long as the Mach line originating at the trailing edge of the root chord does not cross the leading edge. Then, using the results of references 7, 10, or 13,

$$k_a = 1 - \frac{S_T}{S} \quad \frac{\pi m \sqrt{1-m^2}}{\sqrt{M_0^2-1}\,(dC_L/d\alpha)\,E^2} \tag{14}$$

where S_T is the area of the triangular wing having the same leading edge, and E is the complete elliptic integral of the second kind for the modulus $\sqrt{1-m^2}$. For a swept-forward wing with a subsonic leading edge, the theoretical leading-edge suction has not been evaluated.

Before leaving consideration of the drag characteristics, certain properties of the theoretical equations may be noted. Since the lift-curve slope of flat surfaces of the type employed in the present analysis of camber is unaltered by a reversal of the direction of flight (p. 9), the components of minimum drag given by equations (6) and (8) will exhibit the same independence. The remaining pressure component of minimum drag, the drag due to thickness C_{D_t}, is also known to have the same property. It follows that the minimum pressure drag of the wings for which it was calculated is symmetrical with respect to angle of sweep. This result can readily be shown to hold, not only for wings of the present section, but for any wing having a curved camber surface generated by a straight line, the sweep angle of which is always less than that of the Mach cone. In a similar manner, it follows from equation (9) that the theoretical lift coefficient for minimum drag is antisymmetrical with respect to angle of sweep, and that the straight wing U-2 will have its theoretical minimum drag at zero lift.

For the wings for which the effects of camber were analyzed - that is, all except SB-3 and SF-3 - it was found that the components of minimum drag $C_{D_{cc}}$ and C_{D_t} were equal within the limits of computational accuracy. It can be shown that this equality is, in fact, exact for the wings in question. Since the component of

minimum drag given by equation (8) is relatively small in each case, this means that the introduction of camber here has the effect of approximately doubling the calculated minimum pressure drag for the wings with supersonic edges.

Section Characteristics by Higher-Order Theories

The linear theory used in the foregoing calculations is, by virtue of its assumptions, a first-order theory in the perturbation velocity. It is useful, before proceeding to the experimental results, to consider the possible effects of the higher-order terms neglected in this simplified theory. The matter can be approached by studying the two-dimensional case. It is then possible to compare the results of the linear theory with those of the second-order theory of Busemann (references 14, 15, and 16) and of the still more accurate shock-expansion method (reference 17). For the present airfoil section, the last method gives, in fact, the complete inviscid solution at moderate angles of attack. The characteristics of the present isosceles-triangle section as calculated by each of the three theoretical methods are listed at the bottom of table II, which appears at the end of the report. (It may be remarked that the shock-expansion method gives curves which deviate slightly from the perfect straight-line or parabolic shapes given by the other theories.)

The various theoretical section characteristics of table II are seen to fall into two groups, according to whether or not there is an improvement in accuracy in going from the linear to the more refined theories. Thus the linear theory gives a very close approximation for the lift-curve slope, moment at zero lift, minimum pressure drag, and increase in pressure drag with increase in lift. (The quantities concerning the derived curve of lift-drag ratio are not important here.) Going to the second-order approximation provides a noticeable improvement in the calculation of the angle of zero lift, moment-curve slope, and lift coefficient for minimum drag, quantities for which the linear theory gives identically zero. In moment-curve slope, for example, the improvement is equivalent to a shift in aerodynamic center of approximately 3 percent of the mean aerodynamic chord. The foregoing conditions are typical of airfoils in two-dimensional flow.

The discrepancy in the calculated position of the aerodynamic center merits further examination. For a straight-line moment curve, the displacement δ_r of the aerodynamic center forward of any

arbitrary reference point is defined in terms of the mean aerodynamic chord by the equation

$$\frac{\delta_r}{\bar{c}_a} = \frac{dC_{m_r}}{dC_L} = \frac{C_{m_r} - C_{m_{r_{L=0}}}}{C_L} \tag{15}$$

where the moment coefficients are taken about the reference point in question. In general, the lift and moment coefficients in this equation may be expanded as power series involving quantities of the order ϵ, where ϵ is the airfoil thickness ratio or angle of attack in radian measure.[4] It can be shown that the first term in the series for the lift coefficient C_L is necessarily of order ϵ. Assume that the difference in moments $C_{m_r} - C_{m_{r_{L=0}}}$ is calculated to the same order of accuracy. The possible error in this quantity will then be of the order ϵ^2. Because of the division by C_L, however, the resulting error in the position of the aerodynamic center is only of the first order in ϵ. In other words, calculations by a first-order theory are inherently subject to an error of the first order in the computed position of the aerodynamic center. This is borne out by the results for the present airfoil section, where the error of about 0.03 in the linear calculation is seen to be of the same order as the airfoil thickness. It can be shown, in fact (see equations of reference 16), that the discrepancy in dC_m/dC_L between the first- and second-order theories is for any airfoil section directly proportional to the area of the section. The discrepancy is thus essentially a thickness effect and does not disappear with the elimination of camber.

For wings in three dimensions, rigorous evaluation of the aerodynamic coefficients can be carried at present only as far as the first-order terms given by the linear theory. Here, in contrast to the two-dimensional case, the first-order terms in the expressions for $\alpha_{L=0}$, $C_{L_{D=min}}$, and dC_m/dC_L (for moments about the centroid) are not identically zero. Their numerical value may be large or small depending upon the plan form and airfoil section. The possible error due to the omission of the second-order terms will, however, still be of the same magnitude as that calculated for the respective

[4] The quantity ϵ may also be thought of in terms of the flow field about the wing as the ratio of the perturbation velocity to the free-stream velocity.

quantities in two-dimensional flow. The above reasoning with regard to aerodynamic-center position applies, in fact, in three as well as two dimensions. Until more precise solutions become available, therefore, the linear theory should be used with caution in the three-dimensional case for quantities which it does not predict precisely in two dimensions.

RESULTS AND DISCUSSION

Experimental values of lift, drag, and pitching moment for the seven wings are presented in coefficient form in figure 4. The coefficients are referred to the plan-form area of the wings, including the portion of the plan form enclosed by the support body. Pitching moments are taken about the centroid of the plan-form area with the mean aerodynamic chord as the reference length. All the results presented are for a Mach number of 1.53 and a Reynolds number of 0.75 million based on the mean geometric chord of the wing. Theoretical curves obtained as described in the preceding section are included in figure 4 for each case in which they were calculated. The curves shown for the drag coefficient and lift-drag ratio include the pressure drag only and assume no leading-edge suction on any of the wings.

The results of figure 4 are summarized in table II at the end of the text. In each instance, the value determined from the faired experimental curve is given first and the corresponding theoretical value indicated in parentheses directly below.

The results of figure 4 are also cross-plotted against the sweep angle of the midchord line in figures 5 to 9. For reference, both the experimental and theoretical values used in these cross plots are indicated as discrete points. In the case of the experimental quantities, the points shown represent values determined from a faired curve and not actual test points. Where the theoretical curves extend between 43° and 60° in either the swept-back or swept-forward case, the shape of the curve is only approximate. Strictly, small discontinuities in slope would be expected in these curves at $\pm 43^\circ$ and $\pm 55^\circ$, where the leading edge or trailing edge of the plan form coincides with the Mach cone. No attempt has been made to determine these discontinuities, the theoretical curves being faired smoothly between the available calculated points.

All of the preceding results are for the wings in the sharp-edged condition. No results are included for the tests of wing SB-3

with the leading edge rounded. (See description of models.) As discussed in the consideration of drag rise, this rounding had no discernible effect upon any of the aerodynamic characteristics.

It should be remembered throughout the succeeding discussion that the experimental results are in each case for a wing–body combination, while the theoretical characteristics are for the wing alone. As explained in Part I (p. 10), the effect of the slender support body used here is probably small insofar as the experimental lift and moment are concerned. It may, however, be considerable with regard to the minimum drag. The latter results must therefore be regarded as primarily of qualitative significance in comparison with the theoretical values.

Lift

The experimental lift curves of figure 4 are, except in the case of wing SB–3, essentially linear up to angles of attack of 5°. The slope and intercept values given in table II are thus sufficient to define the curves at the small angles for which the linear theory is most likely to be valid. Above 5°, certain of the wings, notably U–2 and SF–3, exhibit an increasing lift–curve slope with increasing angle. For wing SB–3, the nonlinearity of the lift curve is such that no single value of the slope is significant.

Lift–curve slope.– The nature of the agreement between theory and experiment for the lift–curve slope at small angles is apparent in figure 5(a). For the range of sweep angles from 0° to 60° sweep–forward, experiment and theory are virtually coincident. For the swept–back wings of 30° and 43° sweep, the experimental slopes fall definitely below the theoretical. For the wing of 60° sweep–back, the measured slope at zero lift is greater than the theoretical, although the average slope for this wing is slightly less than theory (0.037 as compared with 0.040). As a result of the differences noted, the experimental variation shown in figure 5(a) is not, as theory would predict, completely symmetrical with respect to direction of sweep. Except for portions of the lift curve of wing SB–3, the swept–back wings show generally lower lift–curve slopes than their swept–forward counterpart. The same condition was observed for the three wings of triangular plan form discussed in Part I (reference 1, p. 21).

The reason for the generally lower slope for the swept–back wings is not clear, although various causes may be suggested as follows:

(a) Support-body interference.- The upwash field about the support body at angle of attack will affect the lift-curve slope to some extent. Since the outboard portions of the wings moved progressively rearward in this field as the plan form varied from swept-forward to swept-back, the resulting effect might be expected to differ generally for the two classes of wings. The direction and extent of the asymmetry due to this cause is, however, difficult to assess.

(b) Wing twist.- The elastic twist of the wings under load, as described in the section on Corrections and Precision, would be expected to increase the lift at a given experimental angle of attack for the swept-forward wings and decrease it for the swept-back wings. This would produce a relative condition of the type observed in the lift-curve slope. Rough estimation of the magnitude of this effect indicates that it could account for a considerable part of the measured differences.

(c) Detachment of the leading-edge wave.- At supersonic speeds, the flow at the sharp leading edge of an unswept wing is characterized by an attached, oblique shock wave, provided the thickness ratio and angle of attack are not excessive. As the sweep angle increases from zero in either direction, however, a condition is eventually reached where the shock wave will detach and move forward of the leading edge at all angles of attack. This phenomenon occurs when the Mach number and deflection angle normal to the leading edge satisfy the conditions for detachment of a shock wave from a wedge in two-dimensional supersonic flow. For a family of tapered wings, this condition is attained at different values of the midchord sweep angle in the swept-forward and swept-back cases. For the present wings, the theory of oblique shock waves indicates that the wave will detach from the leading edge throughout the angle-of-attack range at midchord sweep angles of $-46\frac{1}{2}^\circ$ and $+31\frac{1}{2}^\circ$, respectively. This detachment will affect all aerodynamic characteristics of the wings in a way which is outside the scope of the linear theory and may contribute to the observed asymmetry in the lift-curve slope.

(d) Interaction between shock wave and boundary layer at trailing edge.- The theoretical inviscid flow over a lifting airfoil section at supersonic speeds is also marked by an oblique compression wave originating on the low-pressure surface at the trailing edge. As shown in two-dimensional tests by Ferri (reference 18), this pattern is modified in the real

case by an interaction between this trailing wave and the boundary layer on the airfoil surface. The boundary layer separates from the surface some distance ahead of the trailing edge, with the formation of a compression wave at the separation point and a loss of lift between this point and the trailing edge. Since the magnitude of this effect is roughly proportional to the angle of attack, the net result is that the measured lift-curve slope is less than the value given by inviscid theory.

A similar interaction is to be expected at the trailing edge of a swept wing when that edge is supersonic. As with the shock-wave detachment from the leading edge, however, the effects of this interaction may be different for corresponding swept-forward and swept-back wings. This would follow from differences in the length and sweep angle of the trailing edge and in the deflection angle of the flow normal to the edge. The situation would also be complicated by possible differences in the spanwise boundary-layer flow which is to be expected on a swept wing.

Since all of the foregoing phenomena will affect the absolute as well as the relative values of the lift-curve slope, the almost exact agreement between experiment and linear theory for the swept-forward wings should not be taken literally. Shock-wave, boundary-layer interaction, for example, would be expected to cause a decrease in the experimental slope as compared with the theoretical. On the other hand, wing twist in the swept-forward case would cause an increase in slope, and support-body interference would probably do likewise. These effects may be completely compensating on the swept-forward wings.

Angle of zero lift.- As seen in figure 5(b), the experimental values of the angle of zero lift are consistently higher than those predicted by the linear theory.

Examination of the experimental and theoretical values for the unswept wing suggests that this general difference is due mainly to the higher-order pressure effects neglected in the linear calculations. For this wing, the theoretical first-order effects of plan form are small, the linear theory giving a zero-lift angle of -0.12° as compared with the value of zero indicated by the same theory for the airfoil section in two-dimensional flow (see bottom of table II). In contrast, the experimental value of 0.4° for the unswept wing is essentially equal to the value computed for the airfoil section by the second-order theory. The fact that the difference of 0.52° between

experiment and linear theory for the complete wing is slightly greater than the effect of the second-order terms for the airfoil section is undoubtedly due to the additional effect of shock-wave, boundary-layer interaction at the trailing edge as previously described. On a cambered section, such interaction will predominate on the upper surface even at small angles of attack. The resulting increase in pressure near the trailing edge leads to a slightly higher angle for zero lift than would be the case in an inviscid fluid. This effect was originally observed by Ferri in reference 18.

As the angle of sweep increases in either direction (fig. 5(b)), the theoretical first-order effects of plan form become more pronounced causing the calculated zero-lift angle to decrease, though not quite symmetrically. The experimental values are seen to exhibit the same general type of variation. For the wings of $\pm 60^{\circ}$ sweep, where the leading edge is swept well inside the Mach cone, the zero-lift angle is definitely negative, as for a positively cambered airfoil at subsonic speeds. This condition has previously been observed for a swept-back wing of triangular plan form in Part I.

Pitching Moment

Although the moment data of figure 4 exhibit a certain amount of nonlinearity, the experimental pitching-moment curves for all of the wings have been drawn as straight lines. Curves faired more precisely through the experimental points would show a consistent upward curvature passing through zero lift with a disappearance or reversal of this curvature at the higher lift coefficients. In Part I of this series (reference 1, p. 23), a variation of this type was indicated in the moment curves for two swept-back triangular wings of uncambered section. Such an indication is, of course, unwarranted, since curvature in the moment curve at zero lift is not possible for an uncambered wing if the test conditions are perfect. It is apparent that there is a small, consistent inaccuracy in the pitching-moment determination in the vicinity of zero lift, probably as the result of small inaccuracies in the pitching-moment strain gage in this region. For this reason, only the average slope of the experimental moment curves is of significance in the general analysis. This average, as taken from the faired straight lines of figure 4, is given in table II, together with the value of the moment at zero lift.

Moment-curve slope.- The relationship between the average moment-curve slope given by experiment and the slope calculated

by the linear theory is shown in the cross plot of figure 6(a). Here the slope may be regarded as an approximate measure of the displacement of the aerodynamic center from the centroid of plan-form area taken positive toward the leading edge and expressed as a fraction of the mean aerodynamic chord. The experimental results of figure 6(a) show a variation in the position of the aerodynamic center with change in sweep angle which is opposite to that predicted by the linear theory. For the range of sweep angles calculated, theory indicates a progressively forward movement from negative to positive positions as the plan form changes from swept-forward to swept-back. The experimental positions lie always ahead of the centroid and move generally rearward as the sweep angle increases algebraically. The magnitude of the disagreement between theory and experiment is considerable, reaching a maximum of 17 percent of the mean aerodynamic chord for wing SF-2. Although the experimental values of the moment-curve slope are subject to some error because of the questionable curvature noted in the moment data at zero lift, the disagreement observed here is, in general, too large to be attributed to experimental inaccuracy.

For zero sweep, where most of the wing is operating essentially as an airfoil in two-dimensional flow, the difference of 0.052 between theory and experiment can be accounted for largely by the higher-order pressure effects neglected in the linear theory. As seen at the bottom of table II, the inclusion of the second-order terms will account for a shift of 0.032 in the theoretical slope for the airfoil section alone. The remainder of the difference is attributable to the effect of shock-wave, boundary-layer interaction in reducing the lift near the trailing edge.

The disagreement between the experimental and theoretical variation in aerodynamic-center position with change in sweep is more difficult to explain. Except for the unswept wing just considered, the error introduced in the theoretical calculations by the neglect of the second-order pressure terms cannot yet be estimated with accuracy. It can only be said (see p. 17) that the possible error is, for any wing, of the same order as the percent thickness of the wing section. The differences between theory and experiment in figure 6(a) are generally of this order, but considerable variation of the actual numerical value of the second-order terms would be required to correct the discrepancy over the complete range of sweep angles. In addition to the higher-order pressure effects, the experimental results are also subject to the influences previously mentioned as affecting the variation in lift-curve slope. Shock-wave, boundary-layer interaction near the trailing edge would be expected, for example, to cause a forward shift of the aerodynamic

center on both the swept-forward and swept-back wings, though in differing amounts. Wing twist would do the same, although estimation of this effect indicates that it is of small consequence here. The effects of support-body interference and of nose-wave detachment are difficult to assess. In general, there is need for considerable more research before the moment-curve slope can be predicted with accuracy for a wide range of plan forms. A second-order theory of three-dimensional wings would be of great value in this regard.

Moment at zero lift.- The experimental values of moment at zero lift in figure 6(b) agree reasonably with the predictions of the linear theory, being, in general, slightly less negative. The experimental variation with sweep angle is small throughout the complete range and is almost symmetrical with respect to zero sweep. The theoretical variation is likewise nearly, though not exactly, symmetrical over the range in which it could be determined. In view of the theoretical results for the airfoil section in table II, it is not likely that the small discrepancies that do exist between theory and experiment are attributable to second-order pressure effects. The relative displacement of the experimental values in the positive direction is, in fact, consistent with the occurrence of shock-wave, boundary-layer interaction on the upper surface near the trailing edge as described in the previous discussion of angle of zero lift.

Drag and Lift-Drag Ratio

Analysis of the data indicates that the experimental drag curves of figure 4 have in each case an approximately parabolic shape as predicted by equation (3). The curves are thus completely defined by the minimum drag coefficient $C_{D_{min}}$, the lift coefficient for minimum drag $C_{L_{D=min}}$, and the drag-rise factor $\Delta C_D/(\Delta C_L)^2$. The measured values of these quantities for the present wings are listed in table II, together with other pertinent information concerning the drag and the derived curves of lift-drag ratio. The comparable theoretical values in the table were computed by consideration of the pressure drag alone, and the theoretical effects of leading-edge suction on wings SB-3 and SF-3 have been disregarded.

Minimum drag.- Although the presence of the support body precludes a detailed comparison between experiment and theory with regard to minimum drag, several important facts are evident in the cross plot of figure 7(a). Somewhat surprisingly, the experimental variation of minimum drag with angle of sweep is almost exactly symmetrical about the vertical axis. As the sweep increases from zero in either direction, the measured drag first rises slightly to a peak in the vicinity of the Mach cone and then falls markedly with further increase in sweep. The peak is, however, much less pronounced than the linear theory would indicate.

The manner in which the linear theory overestimates the initial rise in minimum drag as the absolute sweep angle increases from zero is noteworthy. For zero sweep, the measured minimum drag coefficient is 0.0065 greater than the theoretical value for pressure drag alone (table II and fig. 7(a)). The friction drag of the laminar boundary layer which is likely over most of this wing at the present Reynolds number would account for half of this difference, and the remainder could easily be due to the effects of the support body. Similarly the difference between experiment and inviscid theory for the wings of $\pm 30^\circ$ sweep is not improbable considering the uncertainties involved in the friction and support-body effects. For the wings of $\pm 43^\circ$ sweep, however, the measured values of minimum drag are practically equal to the computed values for pressure drag alone. It is, of course, possible that in these instances favorable support-body interference could exist of sufficient magnitude to offset the friction drag. It is also possible that the observed results reflect a fundamental limitation of the linear theory in the prediction of pressure drag for a wing swept near the Mach cone.

This latter possibility is suggested by comparison of the present results with those of Hilton and Pruden (reference 19). In these earlier two-dimensional tests, the measured minimum drag of a sharp-edged airfoil at $M_0 = 1.21$ was found to agree almost exactly with the value calculated from inviscid, linear theory. Because some allowance for friction drag must be made in a real gas, it was inferred from this that the linear theory overestimated the pressure drag of the airfoil section at speeds slightly above the speed of sound. In the present tests, the relationship between experiment and theory observed by Hilton and Pruden is duplicated by wings SB-2 and SF-2. This suggests that the linear theory also overestimates the pressure drag for a finite-span wing when the Mach number normal to the wing elements is only slightly supersonic. The correspondence between the two sets of results leads one to suspect the influence of some phenomenon which exists in both cases but which is outside the scope of the linear theory - as, for example, detachment of the compression wave from the leading edge. Whatever the cause, the experimental reduction of the drag peak for sweep angles in the vicinity of the Mach cone is of importance beyond the present family of wings. On the basis of these results, a similar softening would be expected in the peaks which linear theory predicts in the curves of drag versus Mach number for a given swept wing (reference 13).

The decrease in minimum drag observed in figure 7(a) as the sweep angle of the wing is increased beyond that of the Mach cone has been found in numerous previous tests (see, for example, references 20 and 21) and need not be enlarged upon here. This behavior is in qualitative accord with theory. (In the present case, a quantitative comparison between measured and calculated drags for the 60° sweep wings is not possible because of the undetermined theoretical effects of camber.)

The degree of symmetry in the experimental variation of minimum drag throughout the range of sweep angles is remarkable. According to the previous theoretical considerations, the pressure drag as given by the linear theory is exactly symmetrical with respect to angle of sweep, at least for the wings between sweep angles of $\pm 43^{\circ}$. It is surprising that the experimental results, which do not agree quantitatively with the theory, should also exhibit an almost perfect symmetry. One would expect that differences in the detachment of the leading-edge shock wave and probable inequalities in friction drag between corresponding swept-forward and swept-back plan forms would cause an asymmetry akin to that previously observed in the lift-curve slope. Further research is required to determine whether the symmetry observed here is merely fortuitous or indicative of a theoretical equivalence beyond that predicted by linear theory.

The variation with sweep of the lift coefficient for minimum drag is shown in figure 7(b). As with the moment-curve slope, the linear theory predicts neither the quantitative nor qualitative character of the observed variation. For zero sweep, the experimental value exceeds the theoretical by the same order of magnitude as the difference between the values computed for the airfoil section by the linear and shock-expansion theories. (See table II.) This suggests that the discrepancy throughout the sweep range is due in part to the higher-order pressure effects neglected in the linear theory. It is probably influenced too by the shock-wave, boundary-layer interaction described in the discussion of angle of zero lift.

Drag rise.- The rise in drag as the lift coefficient departs from the value for minimum drag is specified, for a parabolic drag curve, by the value of the drag-rise factor $\Delta C_D/(\Delta C_L)^2$. The theoretical and experimental values of this quantity are cross-plotted in figure 8(a). For wings with a sonic or supersonic leading edge, as is the case for all of the present wings except SB-3 and SF-3, no leading-edge suction is theoretically possible. The drag-rise factor as given by equation (12) then reduces to simply the reciprocal of the lift-curve slope. Between $\pm 43^{\circ}$ sweep, the theoretical curve of figure 8(a) thus reflects the symmetry previously observed for the lift-curve slope in figure 5(a). For the wings of $\pm 60^{\circ}$ sweep, the possible effects of leading-edge suction at the subsonic leading edge must be considered. For wing SB-3, two theoretical values of $\Delta C_D/(\Delta C_L)^2$ are indicated, one assuming zero leading-edge suction as generally supposed for a sharp-edged wing, and one including the full theoretical suction for this plan form. For wing SF-3, only the former value is indicated, since the theoretical suction could not readily be evaluated. For this wing, the spread between the two values would be small anyway, since the leading edge is swept only slightly behind the Mach cone

(fig. 3). The experimental values in table II and figure 8(a) were found, as in Part I, by taking the slope of a straight line faired through the experimental points in a plot of ΔC_D versus $(\Delta C_L)^2$. The departure of the individual points from the straight line was small in each case, indicating that the experimental drag curves have very nearly the theoretically parabolic shape.

Between $\pm 43^\circ$ sweep, experiment and theory agree satisfactorily in figure 8(a), considering the accuracy possible in the determination of the experimental values and the uncertainties introduced by the support body. For wing SF-3, the experimental value agrees with the single point computed on the assumption of zero leading-edge suction. Even if the edge of the wing were not sharp, such a result would be expected in view of the negligible theoretical suction probable on this plan form. For wing SB-3, however, the experimental value of $\Delta C_D/(\Delta C_L)^2$ is noticeably below the theoretical point for zero leading-edge suction. Although considerable reduction in the drag-rise factor is theoretically possible on this plan form as a result of leading-edge suction, the effect is not generally thought to be realizable on a sharp-edged wing.

To examine these results further, it is useful to think of the rise in drag above $C_{D_{min}}$ as caused by a combined rotation and elongation of the vector which represents the accompanying change in resultant force. For a given change in angle of attack from $\alpha_{D=min}$, the value of $\Delta C_D/(\Delta C_L)^2$ varies directly with the rotation and inversely with the length of the vector. The rate of elongation, which is given by the rate of increase of lift, has already been examined in the discussion of lift-curve slope. It remains to consider the relative rotation as defined by the quantity k_a (equation (11)).

Experimental and theoretical values of k_a for the present wings are given in table II and figure 8(b). The experimental values were evaluated in the present report by a different method from that used in Part I. In the earlier report, the evaluation was made by substituting the experimental values of $dC_L/d\alpha$ and $\Delta C_D/(\Delta C_L)^2$ into the theoretical relationship between the three quantities (equation (12) of the present report). This method has not been used here since it, in effect, assumes that the experimental lift and drag curves are exactly a straight line and a parabola, respectively. Instead, an average experimental value of k_a for each wing has been determined, in accord with the definition of equation (11), by taking the slope of a straight line faired through a plot of the observed values of ΔC_D versus

$(\Delta C_L) \times (\alpha-\alpha_{D=min})$. The resulting values of k_a and the previous experimental values of $dC_L/d\alpha$ and $\Delta C_D/(\Delta C_L)^2$ do not necessarily satisfy the purely theoretical relationship of equation (12). The approximation is close, however, for all of the wings except SF-3 and SB-3, which have distinctly nonlinear lift curves. In the absence of leading-edge suction, the theoretical value of k_a for all of the wings is unity - that is, the change in resultant force rotates as if it were fixed rigidly to the wing. For wing SB-3, the value corresponding to the full theoretical suction is given by equation (14) as 0.58.

The experimental values of k_a in figure 8(b) exhibit a relationship with theory like that previously noted for $\Delta C_D/(\Delta C_L)^2$. For the range of sweep angles between $\pm 43^\circ$, where no leading-edge suction is theoretically possible, the observed values do not deviate significantly from unity. The small deviations which do exist are generally in a positive direction. This may be due to support-body effects or, as explained below, to an increase in friction drag with increasing angle of attack. For the sweep angle of -60°, where the theoretical leading-edge suction would be small, the measured value of k_a is also very close to unity. For $+60^\circ$, however, the experimental value lies well below one - in fact, almost halfway toward the theoretical value for full leading-edge suction. This result indicates that the unexpectedly low value of $\Delta C_D/(\Delta C_L)^2$ for wing SB-3 is due to a low rate of rotation of the force vector rather than to a high rate of increase in its magnitude. This is consistent with the results concerning the lift-curve slope for this wing, which indicated that the average rate of elongation of the vector was, if anything, slightly less than that given by theory. (See p. 19)

These results for wing SB-3, though at first surprising for a wing with a sharp leading edge, are consistent with other data from the present investigation and from comparable subsonic tests. In the present tests, however, the over-all situation for the wings with a sharp, subsonic leading edge is still somewhat confusing. Of the three swept-back triangular wings discussed in Part I, all of which had a span and leading-edge sweep angle almost identical with wing SB-3, the two uncambered wings gave values of k_a of 0.86 and 0.95 corresponding to positions of the ridge line at 20 and 50 percent of the chord. Unpublished results for another swept wing with the same section as SB-3 and an only slightly greater sweep angle show a value of 0.84. On the other hand, the results for the third triangular wing of Part I, which also had the same section as wing SB-3, give a value of 1.07. In general, it is difficult to discern any

consistent pattern in these results, although values of k_a less than unity appear to predominate.

The available evidence from two-dimensional subsonic tests of sharp-edge airfoils, however, is more uniform, indicating values of k_a consistently less than unity. The results of reference 22 on double-wedge airfoils of 4- and 6-percent thickness at a Mach number equal to that normal to the leading edge on wing SB-3 ($M_n \cong 0.65$) show values of k_a of the order of 0.6 to 0.7 at lift coefficients below 0.4. Similarly, the results of reference 23 on five double-wedge and circular-arc airfoils at the same Mach number indicate values ranging between 0.7 and 0.9, the values (with one exception) decreasing as the included section angle at the leading edge increases. In view of the agreement of these results from two independent two-dimensional tests, it is not likely that the reduction of k_a below unity for wing SB-3 is due to experimental error. Similarly, it is improbable that it could be attributed to support-body effects or other conditions peculiar to the present test.

Although no satisfactory explanation of the result is known, several possibilities may be mentioned for future study:

(a) Leading-edge suction.- The theoretical forward force on the leading edge might be partially realized even on a supposedly sharp edge, either through the nonlinear effects of wing thickness upon the pressure distribution in the immediate vicinity of the edge, or through the fact that the edge of any real wing must have a small radius of some finite dimension.

(b) Boundary-layer separation.- Increasing separation of the boundary layer with increasing angle of attack would be expected to influence the relative rotation of the change in resultant force by its effect upon both the pressure distribution and the skin friction. For any given wing, the effect upon the pressure distribution might either increase or decrease k_a, depending upon the shape of the wing section, the position of separation, and the nature of the leading and trailing edges - that is, whether they are subsonic or supersonic. The effect upon the skin friction would be to decrease k_a by eliminating the friction drag in the separated region. The magnitude of these effects could be considerable. This is especially true for wings with a sharp, subsonic leading edge where, as observed in the schlieren photographs of reference 23, the flow may be separated over the entire upper surface.

(c) Changes in flow in an unseparated boundary layer.- For a wing with predominately laminar boundary-layer flow at minimum drag (as, for example, wing SBT-2 of Part I), an increase in angle of attack might, if the flow remained unseparated, be accompanied by an increase in the area of turbulent flow on the upper surface and a consequent increase in friction drag. This would be reflected by an increase in k_a above the value predicted by an inviscid theory. For a wing with predominately turbulent flow at minimum drag (wing SBT-1 of Part I), a corresponding decrease in the turbulent area on the lower surface would be expected, causing a reduction in k_a.

In an attempt to reduce the values of k_a and $\Delta C_D/(\Delta C_L)^2$ for wing SB-3, the leading edge was rounded successively to radii of 0.25 and 0.50 percent of the chord. The former value is of the same order as the radius of an NACA low-drag section of comparable thickness ratio. Such rounding had no effect upon any of the aerodynamic characteristics of the wing. This is contrary to the result of Part I, where similar rounding of the leading edge of the swept-back triangle with maximum thickness at 20-percent chord (wing SBT-1) gave a measurable reduction in the drag rise, suggesting an increase in the amount of leading-edge suction being realized. This difference is probably associated, not with the differences in plan form between the two wings, but with differences in the wedge angle at the leading edge. Unfortunately, modifications of the triangular wing with maximum thickness at 50-percent chord, which might have thrown some light on this question, were not included in the tests.

The present results are obviously not conclusive with regard to the question of leading-edge suction on the subsonic leading edge of a highly swept wing. The two-dimensional studies of reference 23 indicate that the flow conditions about such an edge are particularly complex for small leading-edge radii and relatively high Mach numbers normal to the edge. Additional investigation of these flow conditions and of the interrelated effects of leading-edge shape, Mach number, and Reynolds number is required for application in the present problem. On the basis of the present tests, however, rounding of the edge does appear desirable for a leading edge swept reasonably far behind the Mach cone. Such rounding, even though continued in to the root section, has no detrimental effect upon the minimum drag or other aerodynamic characteristics and may be of benefit in reducing the drag rise. The results on wing SBT-1 in Part I and on the NACA 0006-63 and 66-006 sections in reference 23 suggest the use of a section with maximum thickness relatively far forward in order to maintain as large a leading-edge radius as possible with a given thickness.

The final answers to questions of this kind, however, will require much detailed research.

Lift-drag ratio.- For a parabolic drag curve of the general type defined by equation (3), the value of the maximum lift-drag ratio is given by

$$\left(\frac{L}{D}\right)_{max} = \frac{1}{2[\Delta C_D/(\Delta C_L)^2]\,(C_{L_{opt}} - C_{L_{D=min}})} \tag{16}$$

where the corresponding lift coefficient $C_{L_{opt}}$ is given by

$$C_{L_{opt}} = \sqrt{\frac{C_{D_{min}}}{[\Delta C_D/(\Delta C_L)^2]} + C_{L_{D=min}}{}^2} \tag{17}$$

For wings with a moderate amount of camber, the value of $C_{L_{D=min}}$ is small and, since it appears squared in equation (17), has only a secondary effect upon $C_{L_{opt}}$. Its direct effect upon $(L/D)_{max}$ in equation (16), however, is more pronounced. For wings with zero camber, $C_{L_{D=min}}$ vanishes, and the above expressions reduce to equations (17) and (18) of Part I.

Experimental and theoretical values for $(L/D)_{max}$ and $C_{L_{opt}}$ for the present wings are given in table II and figure 9. The theoretical values, which do not include the effects of skin friction, were determined from equations (16) and (17) using the theoretical quantities previously determined. The experimental values were read from the experimental curves of lift-drag ratio in figure 4.

As seen in figure 9(a), the experimental maximum lift-drag ratio varies only between 6 and $6\frac{1}{2}$ over the entire range of sweep angles. The linear theory, on the other hand, predicts a marked decrease in $(L/D)_{max}$ with increase in the absolute sweep angle over the calculated range between $\pm 43^\circ$. This decrease is a

reflection primarily of the corresponding increase in the theoretical minimum drag noted in figure 7(a). The fact that the experimental values of $(L/D)_{max}$ do not follow the theoretical trend is due primarily to the failure of the minimum drag to rise as calculated, and secondarily to the unpredicted shift in the values of $C_{L_{D=min}}$ apparent in figure 7(b). As a result of these two effects, the measured value of $(L/D)_{max}$ for the wings of $\pm 43^{\circ}$ sweep is actually above the theoretical value, which itself would normally be thought to be optimistic since it includes no allowance for friction drag. As the sweep angle is increased to $\pm 60^{\circ}$, for which no theoretical calculations were made, the effect of the experimental decrease in minimum drag noted in figure 7(a) is counterbalanced by the corresponding experimental increase in the drag-rise factor. As a result, the value of $(L/D)_{max}$ is essentially unchanged.

It is apparent from the results of the present investigation that there is a wide field for research in improving the aerodynamic efficiency of wings at moderately supersonic speeds. The theoretical possibilities in this regard have been discussed by Jones (reference 24), whose ideas have contributed greatly to the present study. As is apparent from equations (16) and (17), theoretical and experimental research in this field should be aimed at reducing both the minimum drag and the drag rise and, perhaps, at displacing the minimum drag to as large a positive lift as possible consistent with the other requirements. Lowering the minimum drag implies the attainment of a low thickness drag through the use, insofar as structural limitations will allow, of a high angle of sweep coupled with a relatively high aspect ratio and low thickness ratio. As indicated in Part I, the chordwise distribution of thickness is also of importance in this regard by virtue of its effect upon both the pressure drag and the friction drag. Reducing the drag rise also implies high sweep – that is, a subsonic leading edge – together with a high aspect ratio, in order to take advantage of the leading-edge suction indicated by theory. The requirements as to thickness ratio and distribution necessary to realize the leading-edge suction in practice may, however, conflict with what would be required for lowest minimum drag. The remaining means of benefit – displacement of the minimum drag to a positive lift – can be accomplished through the use of camber. Since camber also tends to increase the magnitude of the minimum drag, however, the net effect upon the lift-drag ratio may or may not be favorable. For wings of low sweep – that is, a supersonic leading edge – the over-all effect of camber would probably be detrimental. For highly swept wings of high aspect ratio, however,

the proper use of camber might, as for an unswept wing in purely subsonic flow, have a net beneficial effect. Although the effect of camber upon the drag-rise factor is theoretically nil in an inviscid fluid, a beneficial effect upon this characteristic might be possible in the real case through the influence of the camber upon the flow conditions at the leading edge and hence upon the amount of leading-edge suction actually realized.

CONCLUSIONS

Tests were conducted at a Mach number of 1.53 and a Reynolds number of 0.75 million of seven wings varying in angle of sweep from 60° sweepforward to 60° sweepback. The wings had a uniform isosceles-triangle section 5-percent thick and a common taper ratio of 0.5. The results afforded the following conclusions:

1. For the unswept and swept-forward wings, the agreement between experiment and linear theory with regard to lift-curve slope was very close. For the swept-back wings, the experimental values were less than the theoretical by 7 to 9 percent (except for the most highly swept wing, where the comparison was complicated by the nonlinearity of the experimental curve). Because of this difference, the experimental slope for a plan form of given shape was not, as theory would suggest, completely independent of the direction of sweep.

2. The experimental angles of zero lift were consistently greater than those given by linear theory by from 0.3° to 0.8° This difference is probably due to the higher-order pressure effects neglected in the linear theory.

3. The experimental values of moment-curve slope indicated a variation of aerodynamic-center position with angle of sweep opposite to that predicted by the linear theory, with individual discrepancies of as much as 17 percent of the mean aerodynamic chord. The discrepancy for the unswept wing was comparable in magnitude to the difference between the theoretical first- and second-order values for the airfoil section in two-dimensional flow.

4. The measured values of the moment coefficient at zero lift were negative throughout the range of sweep angles and agreed reasonably with the values calculated by the linear theory.

5. As the sweep increased from zero in either direction, the measured minimum drag coefficient rose symmetrically to a maximum

for sweep angles in the vicinity of the Mach cone and then fell markedly with further increase in sweep. This type of variation is in accord with the linear theory. The rise in the vicinity of the Mach cone was, however, less pronounced than the theory would indicate.

6. For the wings with a supersonic leading edge, the increase in drag with angle of attack was in accord with theory and indicated that the rearward rotation of the change in resultant force was approximately equal to the accompanying change in angle. For the swept-back wing with a subsonic leading edge, the rotation of the force vector was somewhat less than the change in angle despite the sharp leading edge and presumed absence of leading-edge suction. Rounding the leading edge of this wing had no effect upon this (or any other) aerodynamic characteristic.

7. For the wings considered (isosceles-triangle section), the experimental maximum lift-drag ratio was between the limits of 6 and $6\frac{1}{2}$ over the complete range of sweep angles.

Ames Aeronautical Laboratory,
National Advisory Committee for Aeronautics,
Moffett Field, Calif.

REFERENCES

1. Vincenti, Walter G., Nielsen, Jack N., and Matteson, Frederick H.: Investigation of Wing Characteristics at a Mach Number of 1.53. I - Triangular Wings of Aspect Ratio 2. NACA RM No. A7I10, 1947.

2. Harmon, Sidney M., and Swanson, Margaret D.: Calculations of the Supersonic Wave Drag of Nonlifting Wings with Arbitrary Sweepback and Aspect Ratio - Wings Swept Behind the Mach Lines. NACA TN No. 1319, 1947.

3. Busemann, A.: Aerodynamic Lift at Supersonic Speeds. Rep. No. AeTechl. 1201, British A.R.C., (Translation), Feb. 1937.

4. Puckett, Allen E.: Supersonic Wave Drag of Thin Airfoils. Jour. Aero. Sci., vol. 13, no. 9, Sept. 1946, pp. 475-484.

5. Stewart, H. J.: The Lift of a Delta Wing at Supersonic Speeds. Quart. App. Math., vol. IV, no. 3, Oct. 1946, pp. 246–254.

6. Lagerstrom, P. A., Wall, D., and Graham, M. E.: Formulas in Three-Dimensional Wing Theory. Douglas Aircraft Company Rep. No. SM11901, Aug. 1946.

7. Hayes, W. D., Browne, S. H., and Lew, R. J.: Linearized Theory of Conical Supersonic Flow with Application to Triangular Wings. North Amer. Aviation Rep. No. NA-46-818, June 1947.

8. Cohen, Doris: Theoretical Lift of Flat Swept-Back Wings at Supersonic Speeds. NACA TN No. 1555, 1948.

9. Jones, Robert T.: Thin Oblique Airfoils at Supersonic Speed. NACA TN No. 1107, 1946.

10. von Karman, Theodore: Supersonic Aerodynamics – Principles and Applications. Jour. Aero. Sci., vol. 14, no. 7, July 1947, pp. 373–402.

11. Margolis, Kenneth: Supersonic Wave Drag of Swept-Back Tapered Wings at Zero Lift. NACA TN No. 1448, 1947.

12. Nielsen, Jack N.: Effect of Aspect Ratio and Taper on the Pressure Drag at Supersonic Speeds of Unswept Wings at Zero Lift. NACA TN No. 1487, 1947.

13. Puckett, A. E., and Stewart, H. J.: Aerodynamic Performance of Delta Wings at Supersonic Speeds. Jour. Aero. Sci., vol. 14, no. 10, Oct. 1947, pp. 567–578.

14. Busemann, A., and Walchner, O.: Airfoil Characteristics at Supersonic Speeds. British RTP Translation No. 1786, Forschung., vol. 4, no. 2, Mar./Apr. 1933, pp. 87–92.

15. Lock, C. N. H.: Examples of the Application of Busemann's Formula to Evaluate the Aerodynamic Force Coefficients on Supersonic Airfoils. R. & M. No. 2101, British A.R.C., 1944.

16. The Staff of the Ames 1- by 3-Foot Supersonic Wind-Tunnel Section: Notes and Tables for Use in the Analysis of Supersonic Flow. NACA TN No. 1428, 1947.

17. Ivey, H. Reese, Stickle, George W., and Schuettler, Alberta: Charts for Determining the Characteristics of Sharp-Nose Airfoils in Two-Dimensional Flow at Supersonic Speeds. NACA TN No. 1143, 1947.

18. Ferri, Antonio: Experimental Results with Airfoils Tested in the High-Speed Tunnel at Guidonia. NACA TM No. 946, 1940.

19. Hilton, W. F., and Pruden, F. W.: Subsonic and Supersonic High Speed Tunnel Tests of a Faired Double Wedge Aerofoil. R. & M. No. 2057, British A.R.C., 1943.

20. Ellis, Macon C., Jr., and Hasel, Lowell, E.: Preliminary Tests at Supersonic Speeds of Triangular and Swept-Back Wings. NACA RM No. L6L17, 1947.

21. Tucker, Warren A., and Nelson, Robert L.: Drag Characteristics of Rectangular and Swept-Back NACA 65-009 Airfoils Having Various Aspect Ratios as Determined by Flight Tests at Supersonic Speeds. NACA RM No. L7C05, 1947.

22. Solomon, Joseph, and Henney, Floyd W.: The Subsonic Aerodynamic Characteristics of Two Double-Wedge Airfoil Sections Suitable for Supersonic Flight. NACA RM No. A6G24, 1947.

23. Lindsey, W. F., Daley, Bernard N., and Humphreys, Milton D.: The Flow and Force Characteristics of Supersonic Airfoils at High Subsonic Speeds. NACA TN No. 1211, 1947.

24. Jones, Robert T.: Estimated Lift-Drag Ratios at Supersonic Speed. NACA TN No. 1350, 1947.

TABLE I.- SUMMARY OF GEOMETRIC PROPERTIES OF WINGS

Wing	SF-3	SF-2	SF-1	U-2	SB-1	SB-2	SB-3
Sketch							
$\Lambda_{\frac{1}{2}}$ (deg)	-60.00	-43.00	-30.00	0	30.00	43.00	60.00
Λ_0 (deg)	-54.44	-35.16	-21.03	9.46	37.58	49.25	64.17
Λ_1 (deg)	-64.17	-49.25	-37.58	-9.46	21.03	35.16	54.44
A	2.000	2.924	3.464	4.000	3.464	2.924	2.000
b (in.)	4.242	5.130	5.584	6.000	5.584	5.130	4.242
$\bar{c}_g$ (in.)	2.121	1.755	1.612	1.500	1.612	1.755	2.121
$\bar{c}_a$ (in.)	2.200	1.819	1.671	1.556	1.671	1.819	2.200
x_o (in.)	-0.218	0.105	0.358	1.000	1.791	2.234	3.046
c_r (in.)	2.828	2.339	2.149	2.000	2.149	2.339	2.828

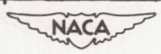

Properties common to all wings:

$(c_t/c_r) = 0.5$

$S = 9$ sq in.

$A = 4 \cos \Lambda_{\frac{1}{2}}$

TABLE II.- SUMMARY OF RESULTS OF FIGURE 4

Wing	Sketch	Lift		Moment		Drag				Lift–drag ratio	
		$\alpha_{L=0}$ [deg]	$\left(\frac{dC_L}{d\alpha}\right)_{L=0}$ [per deg]	$C_{m_{L=0}}$	$\left(\frac{dC_m}{dC_L}\right)_{av}$	$C_{D_{min}}$	$C_{L_{D=min}}$	$\Delta C_D/(\Delta C_L)^2$	k_a	$(L/D)_{max}$	$C_{L_{opt}}$
SF–3		−0.5 (*)	0.0365 (.0400)	−0.037 (*)	0.200 (*)	0.0210 (*)	0.05 (*)	0.425 (.436)	1.02 (1.00)	6.1 (*)	0.25 (*)
SF–2		−.1 (−.88)	.0550 (.0562)	−.052 (−.068)	.126 (−.043)	.0260 (.0242)	.04 (−.006)	.335 (.310)	1.07 (1.00)	6.3 (5.6)	.28 (.28)
SF–1		.3 (−.43)	.0585 (.0582)	−.040 (−.052)	.084 (−.045)	.0250 (.0202)	.04 (−.007)	.320 (.300)	1.10 (1.00)	6.2 (6.3)	.28 (.26)
U–2		.4 (−.12)	.0560 (.0562)	−.033 (−.044)	.064 (.012)	.0240 (.0175)	.02 (0)	.315 (.310)	1.07 (1.00)	6.1 (6.8)	.29 (.24)
SB–1		.1 (−.20)	.0540 (.0582)	−.035 (−.061)	.060 (.021)	.0245 (.0202)	.03 (.007)	.320 (.300)	.99 (1.00)	6.4 (6.6)	.28 (.26)
SB–2		.1 (−.66)	.0510 (.0562)	−.044 (−.070)	.054 (.065)	.0250 (.0242)	.04 (.006)	.320 (.310)	.97 (1.00)	6.5 (5.9)	.28 (.28)
SB–3		−1.0 (*)	.0465 (.0400)	−.040 (*)	.099 (.262)	.0190 (*)	.02 (*)	.365 (.436)	.79 (1.00)	6.5 (*)	.24 (*)
Linear	Section	0	.0603	−.043	0	.0173	0	.289	1.00	7.1	.24
Second order		.36	.0603	−.043	.032	.0170	.011	.289	1.00	7.5	.24
Shock–exp.	Theory	.37	.0615	−.043	.034	.0172	.014	.300	1.00	7.4	.26

Note: For each wing the experimental value is given first and the corresponding theoretical value indicated in parentheses directly below. Where an asterisk is used, the theoretical value has not been computed. The theoretical values for all quantities in the table pertaining to drag and lift–drag ratio include the pressure drag only and assume zero leading–edge suction.

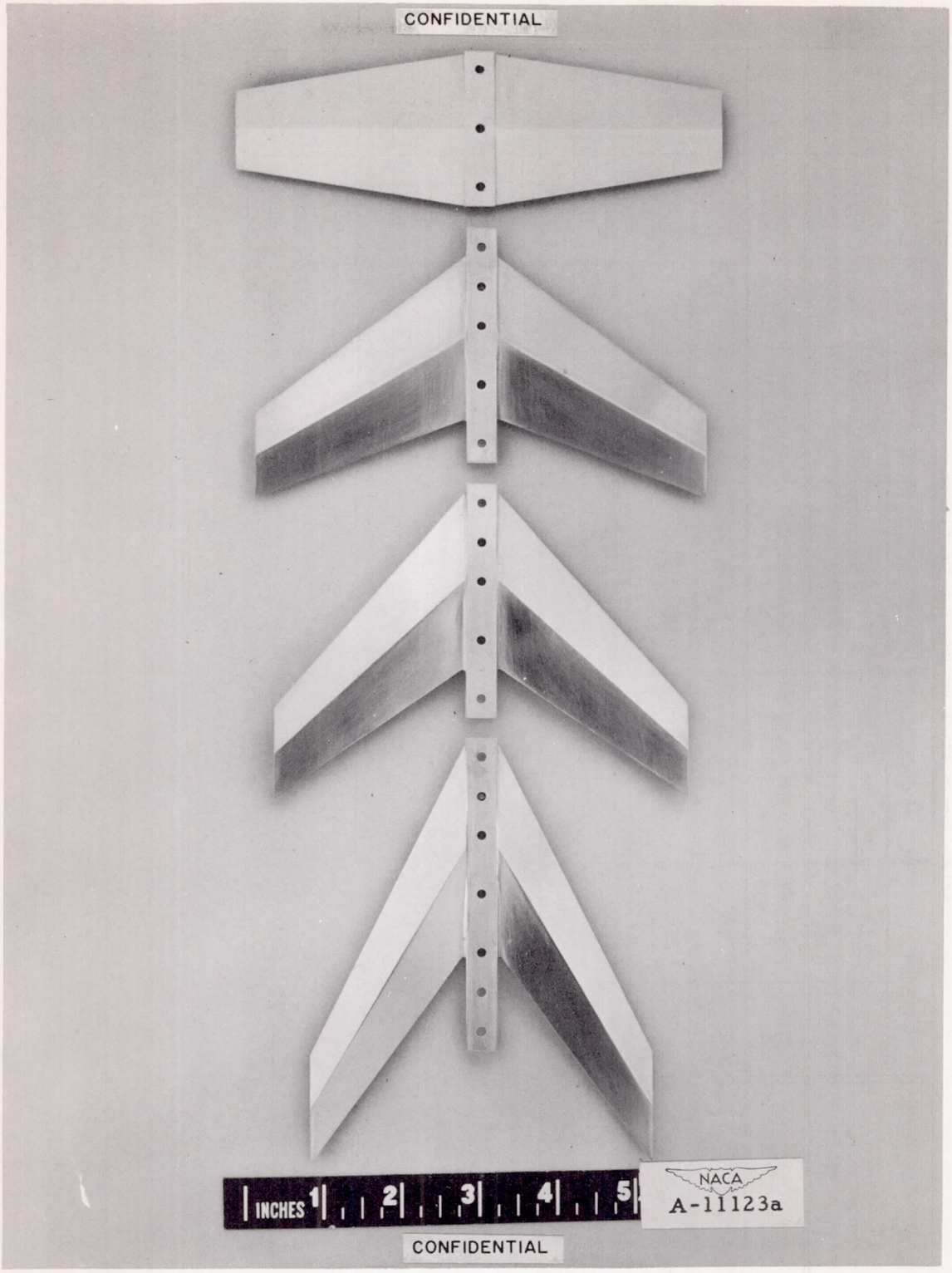

(a) Family of models.

Figure 1.- Test models.

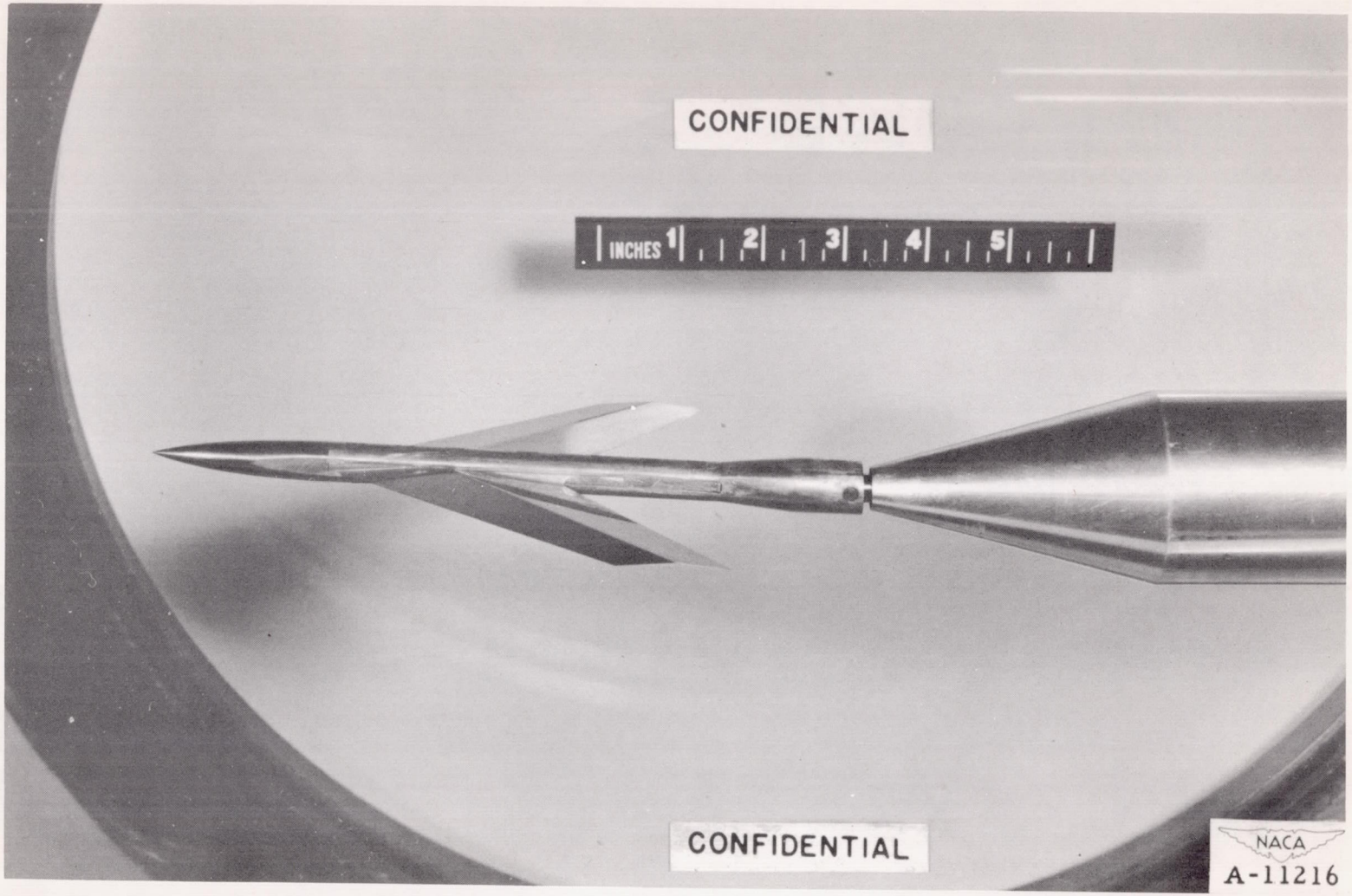

(b) Model mounted in tunnel.

Figure 1.- Concluded.

All dimensions in inches except as noted

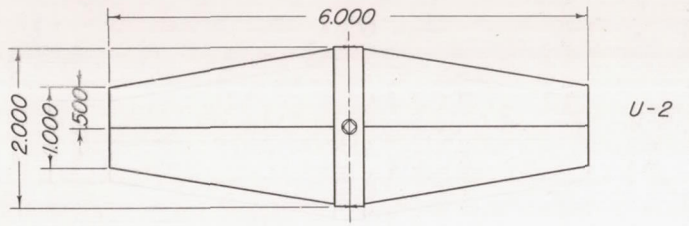

U-2

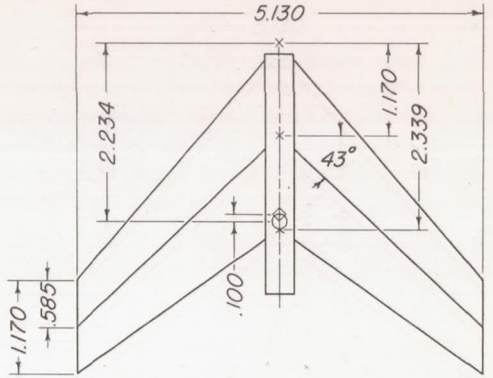

S-2

○ *Centroid of wing plan form*

◇ *Position of body moment reference axis (ref. 1, fig. 3)*

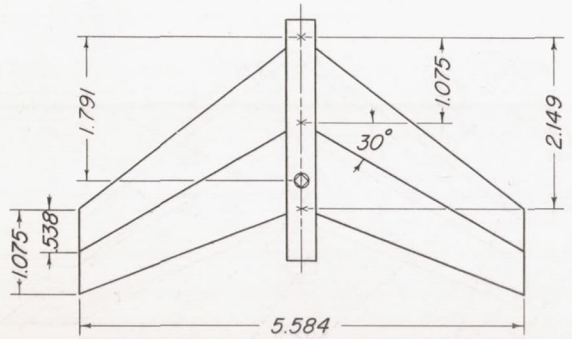

S-1

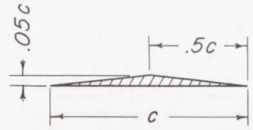

Typical section

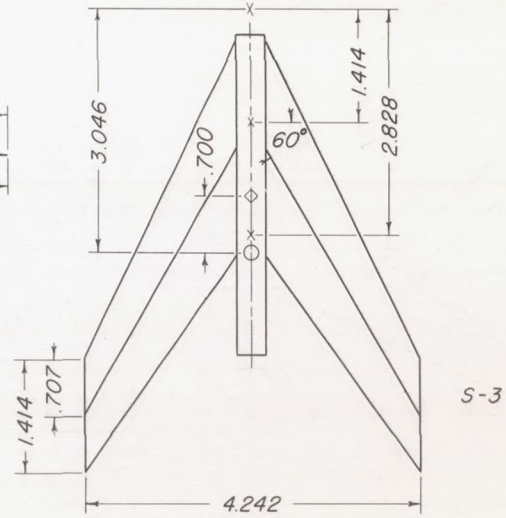

S-3

Figure 2. - Dimensions of models.

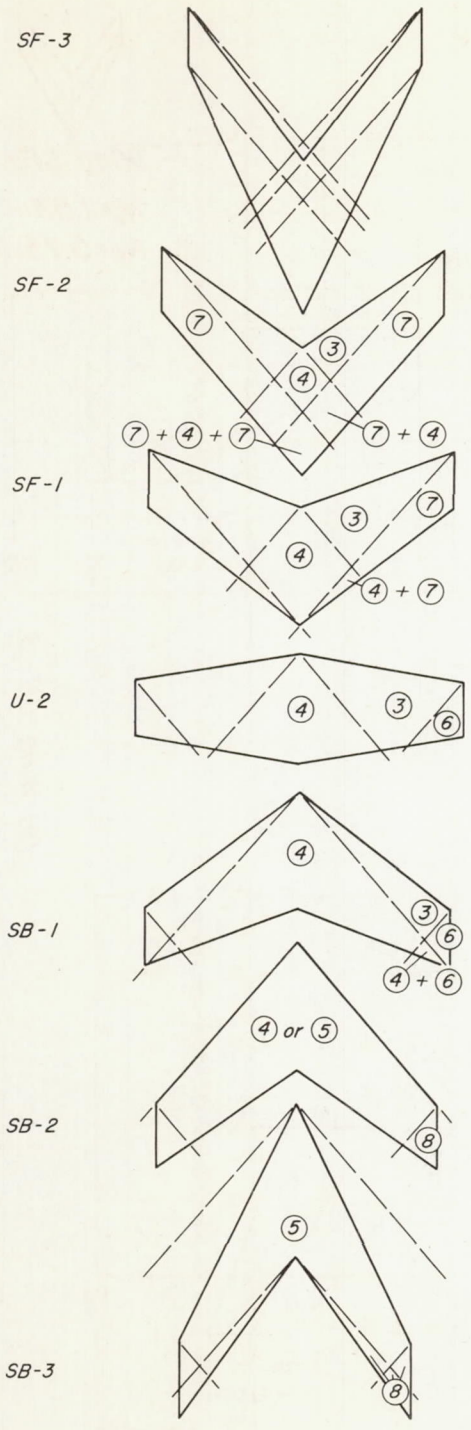

Wing planform

Mach line

Circled numerals indicate reference numbers for the analytical solutions applicable in each region as follows:

③	Busemann	(simple sweep)
④	Puckett	
⑤	Stewart	See list of references for complete title
⑥	Lagerstrom	
⑦	Hayes	
⑧	Cohen	

Where the use of more than one solution is indicated, the total deficiency in pressure below ③ is obtained as the sum of the deficiencies associated with each of the component solutions.

NACA

Figure 3.- Mach-line patterns and pressure fields for flat-plate wings at $M = 1.53$.

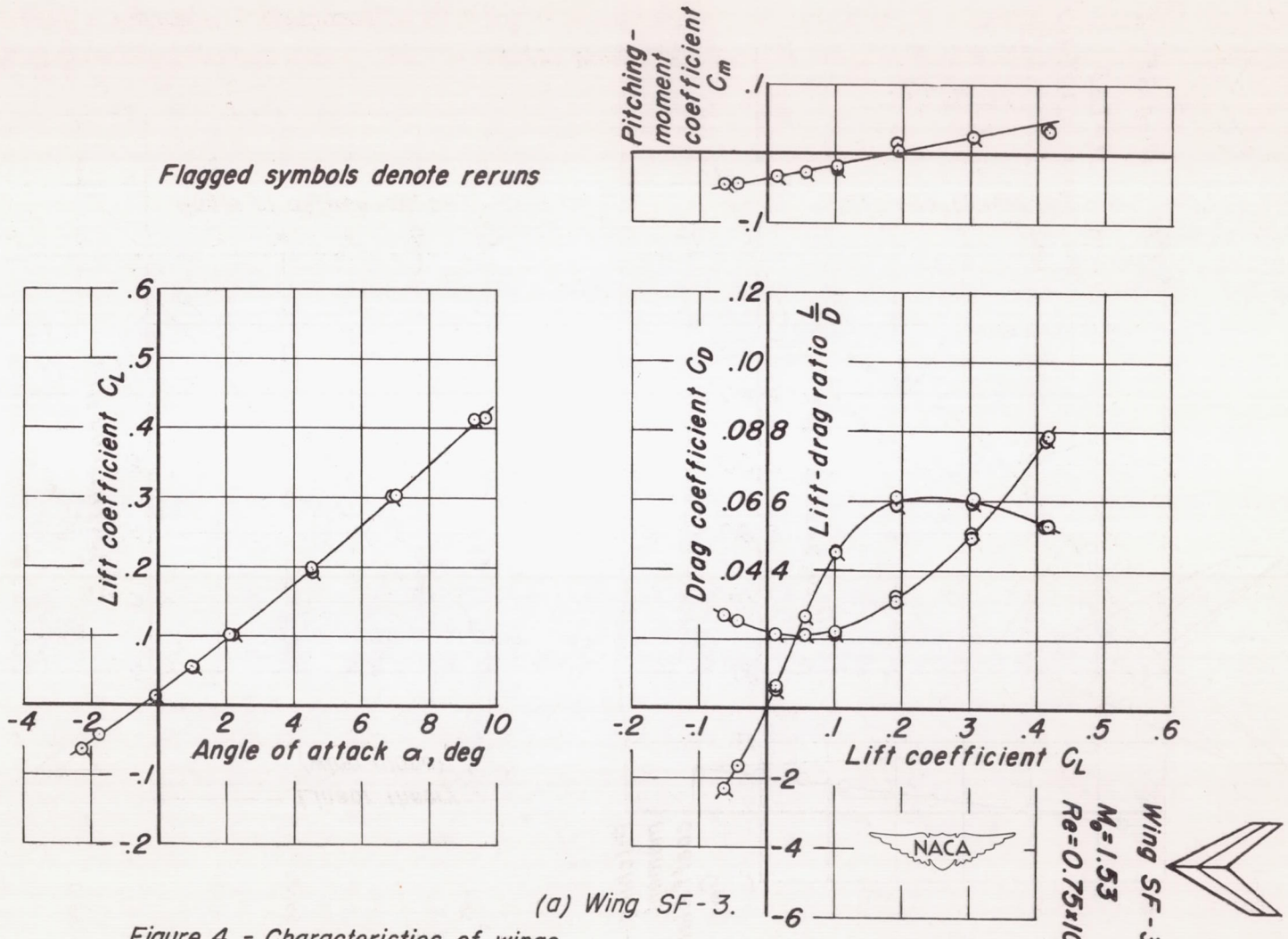

(a) Wing SF-3.

Figure 4.- Characteristics of wings.

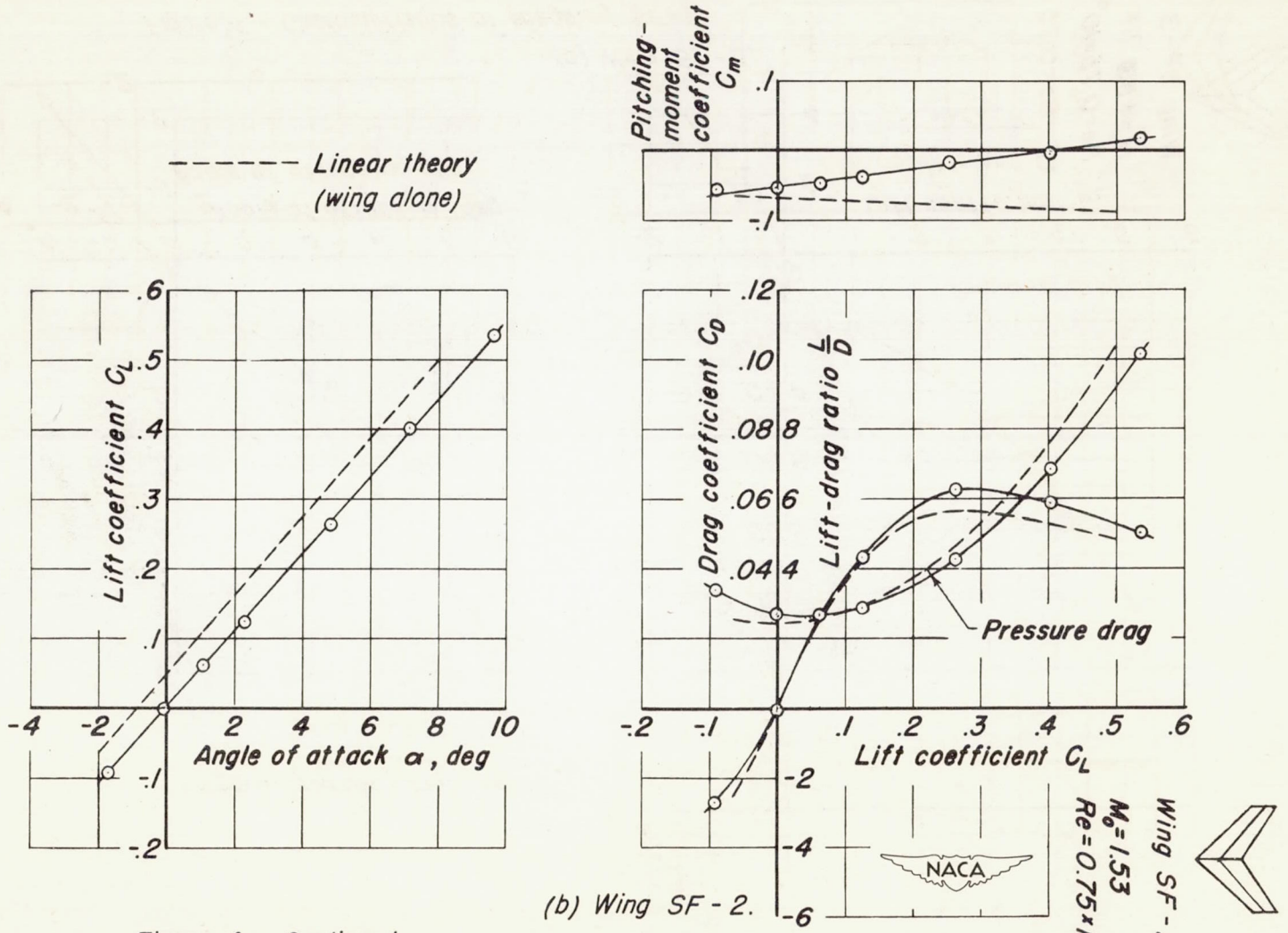

(b) Wing SF-2.

Figure 4.- Continued.

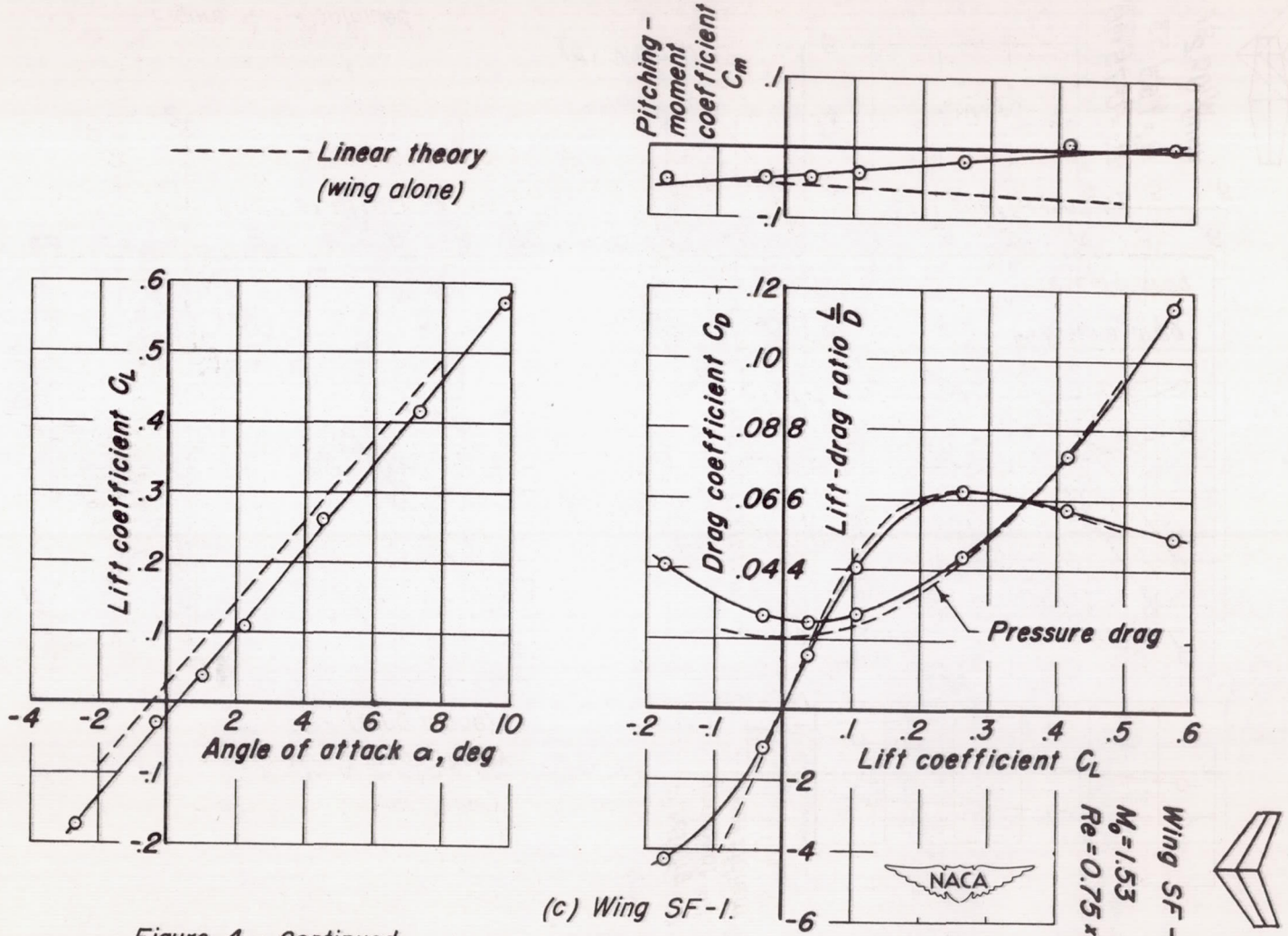

(c) Wing SF-1.

Figure 4.- Continued.

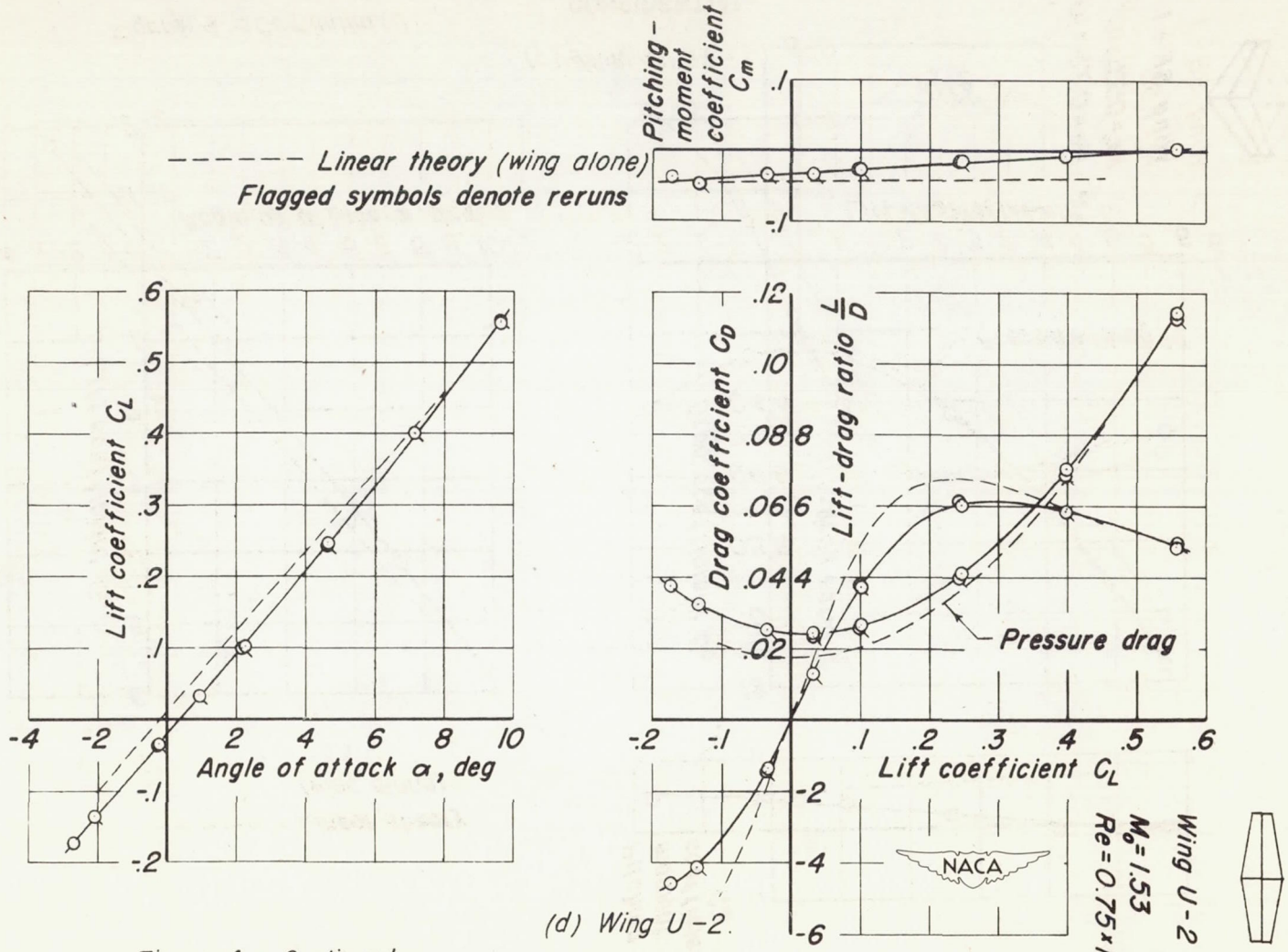

(d) Wing U-2.

Figure 4.- Continued.

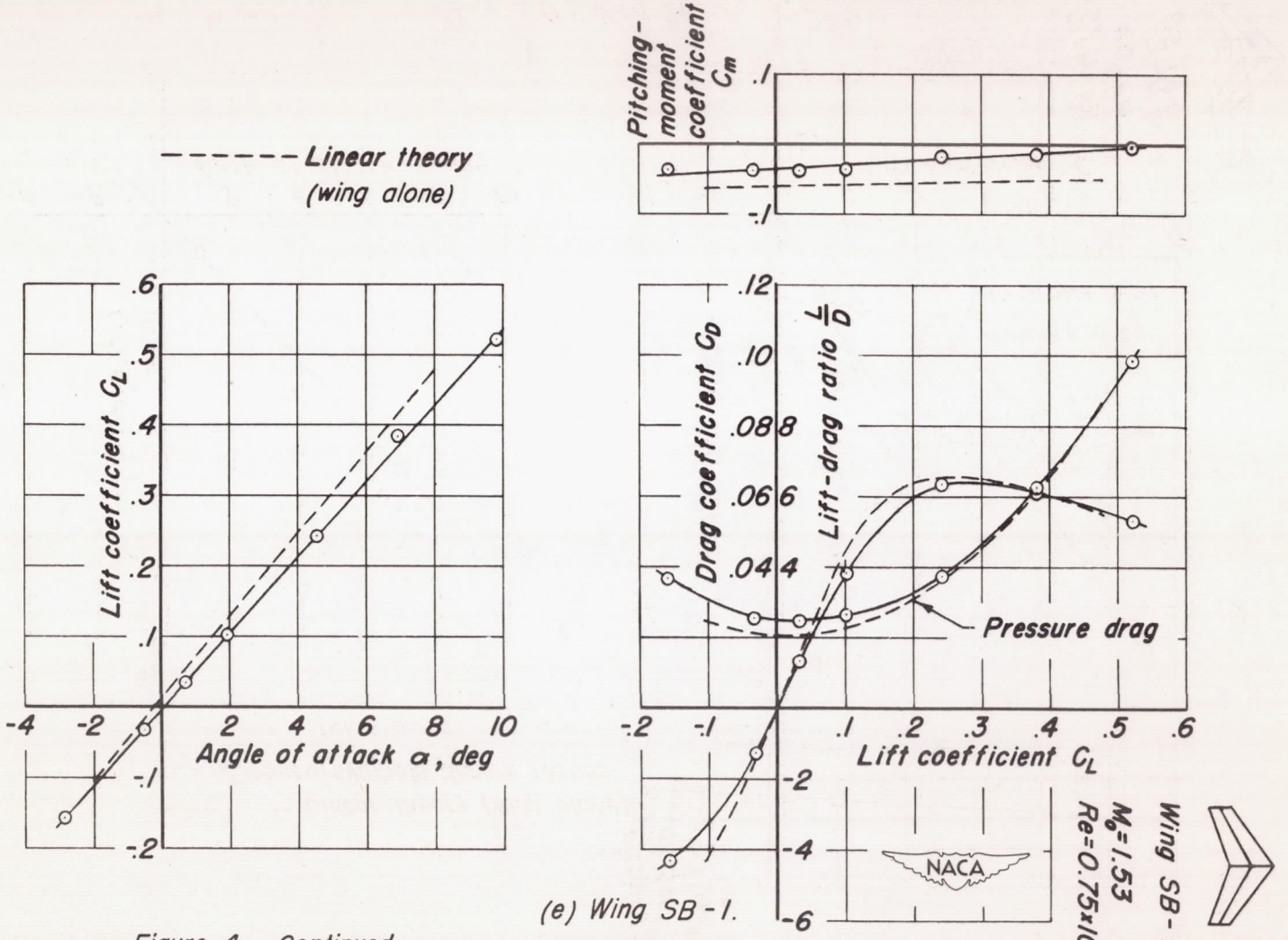

(e) Wing SB-1.

Figure 4. - Continued.

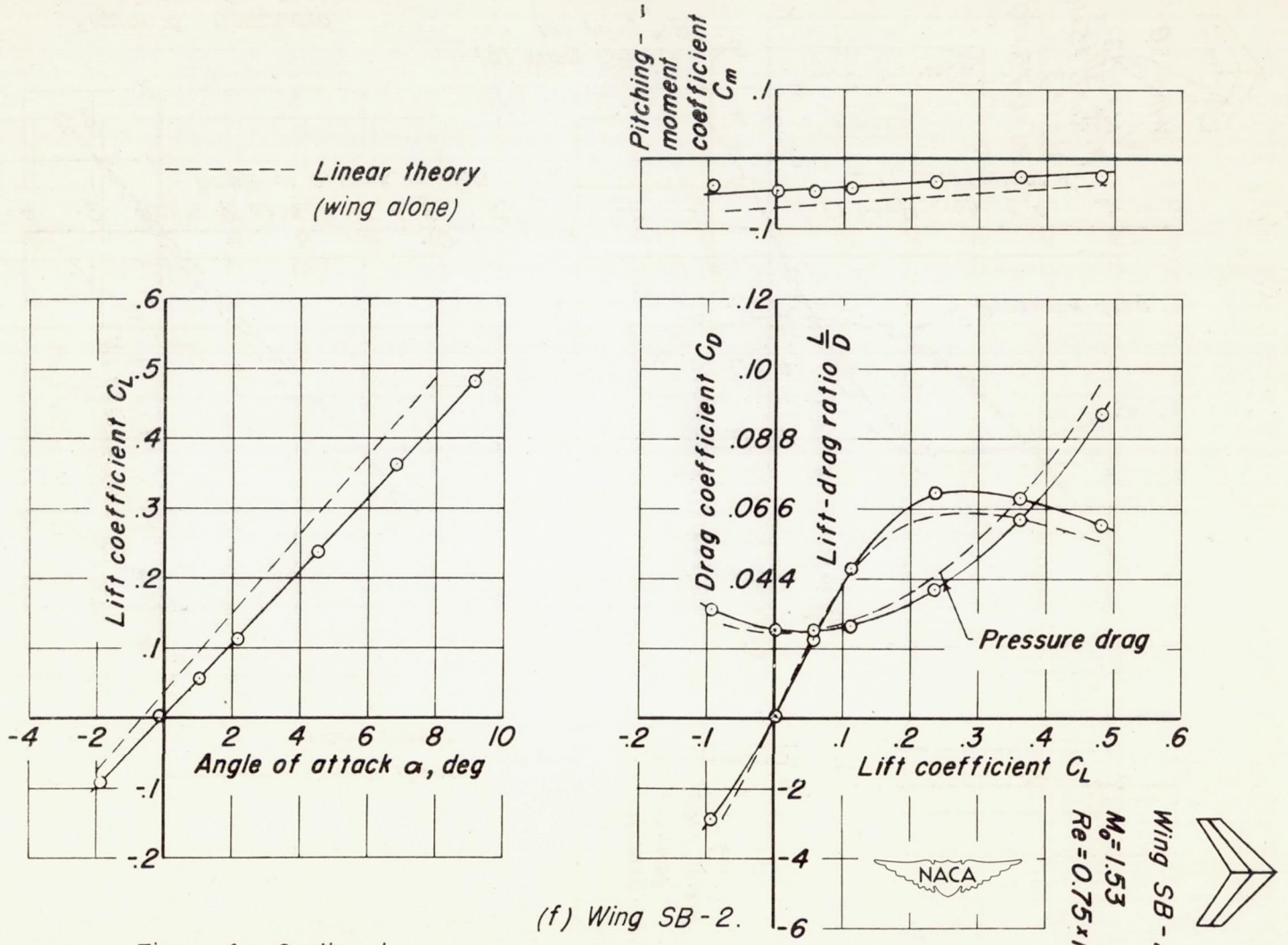

(f) Wing SB-2.

Figure 4.- Continued.

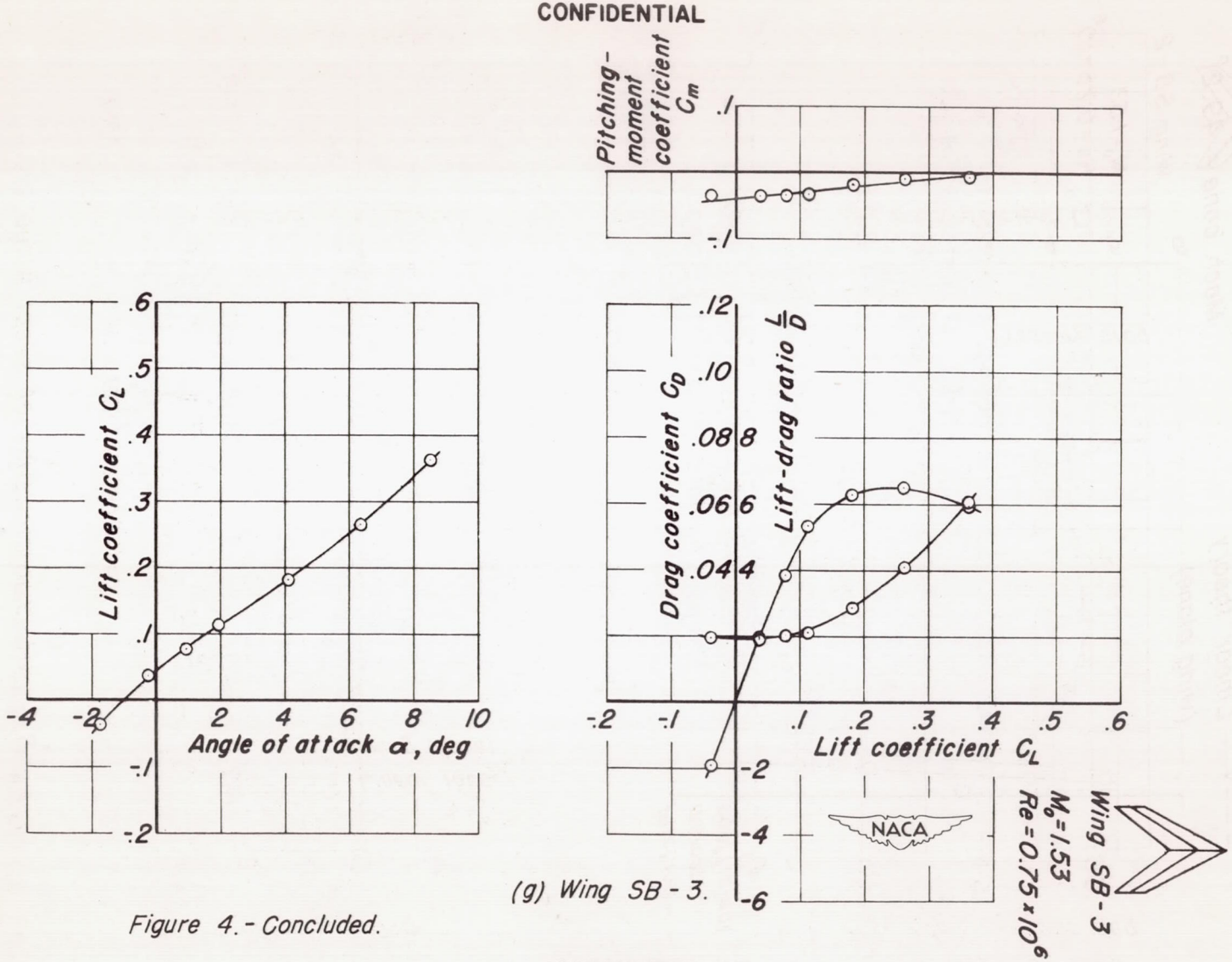

(g) Wing SB - 3.

Figure 4. - Concluded.

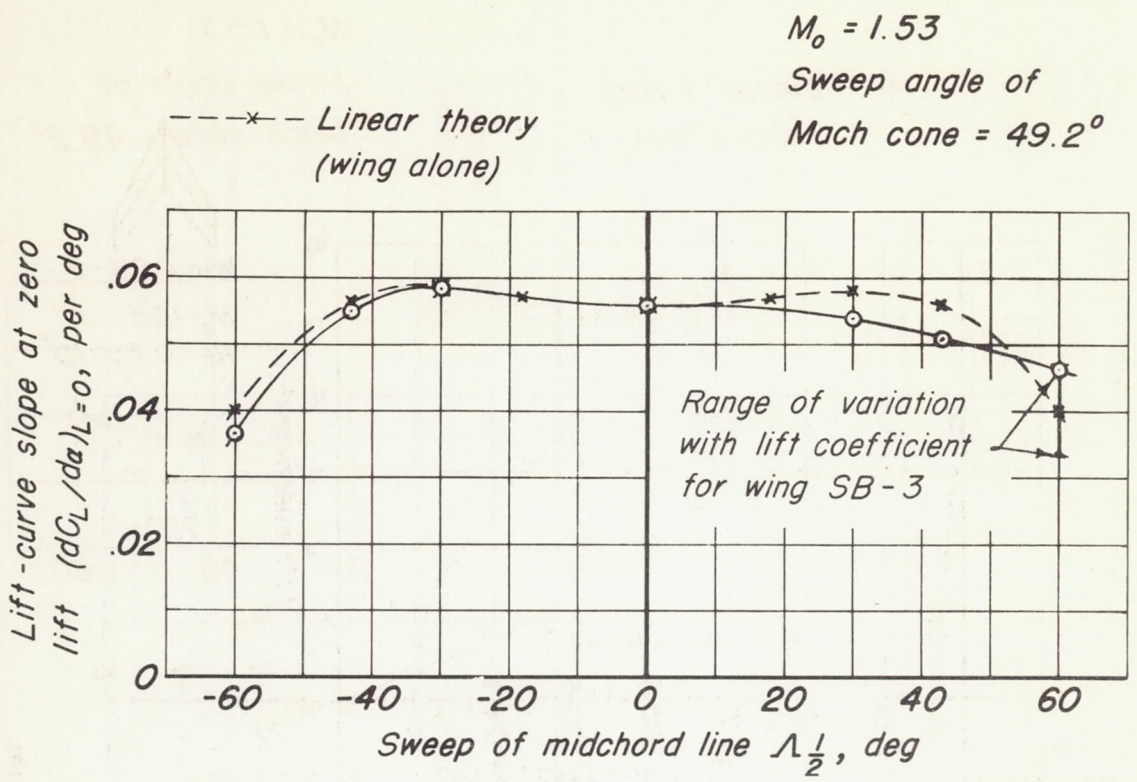

(a) Lift-curve slope.

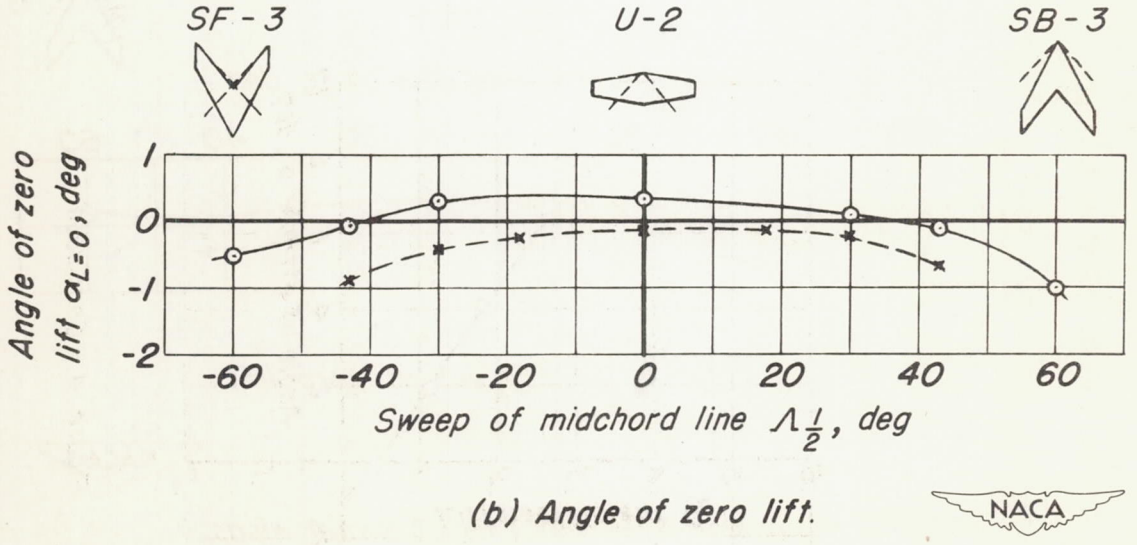

(b) Angle of zero lift.

Figure 5.- Lift characteristics of swept wings.

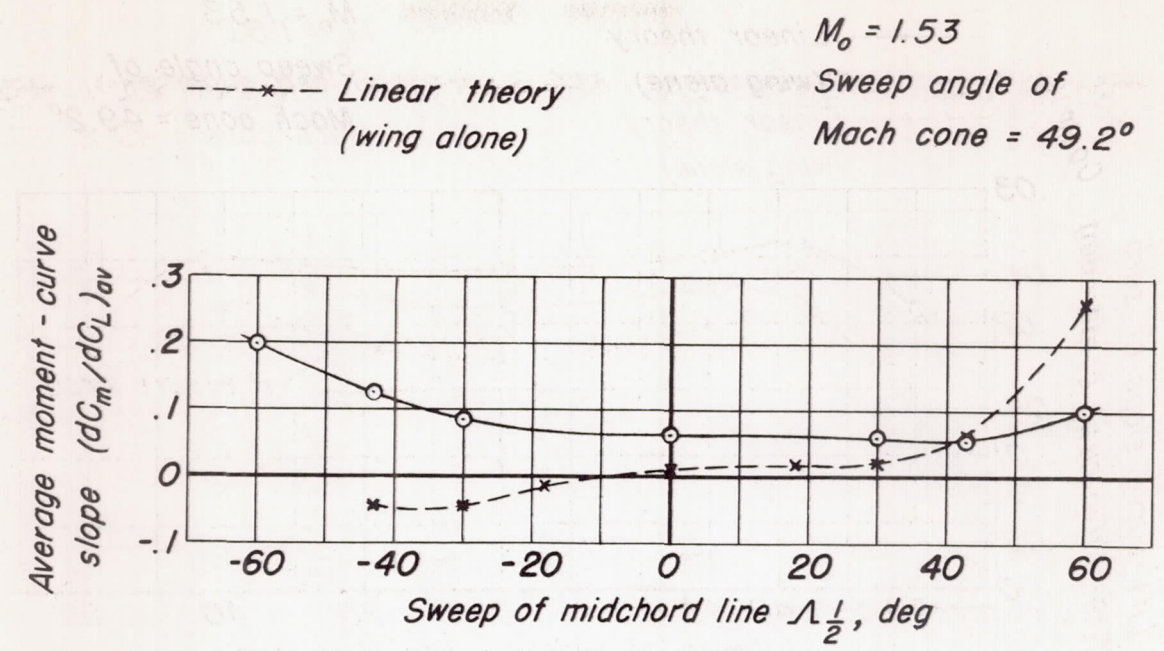

(a) Average moment - curve slope.

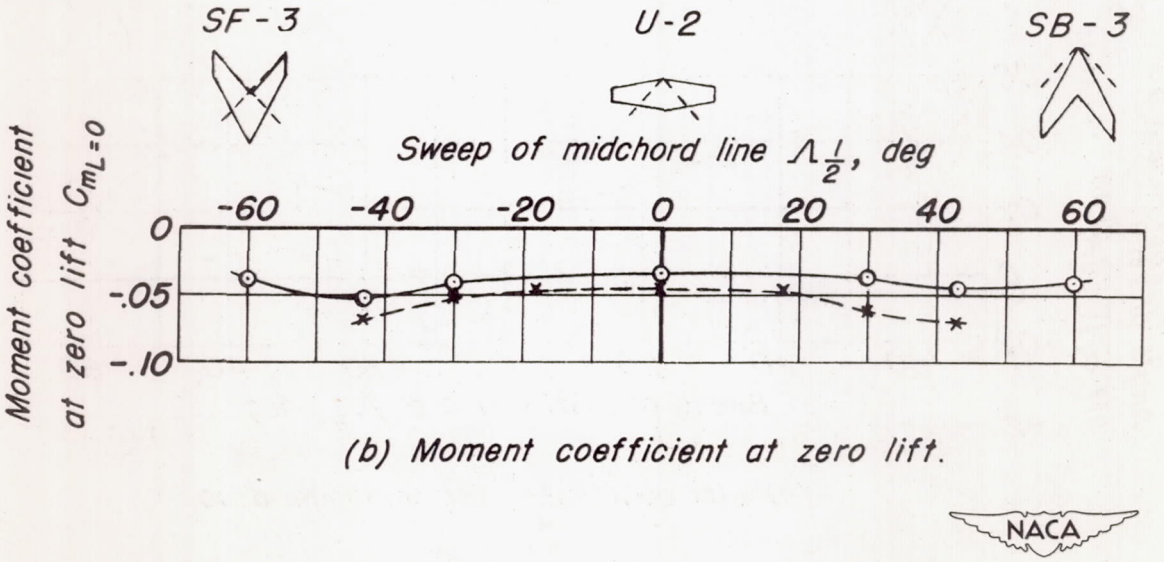

(b) Moment coefficient at zero lift.

Figure 6. - Moment characteristics of swept wings.

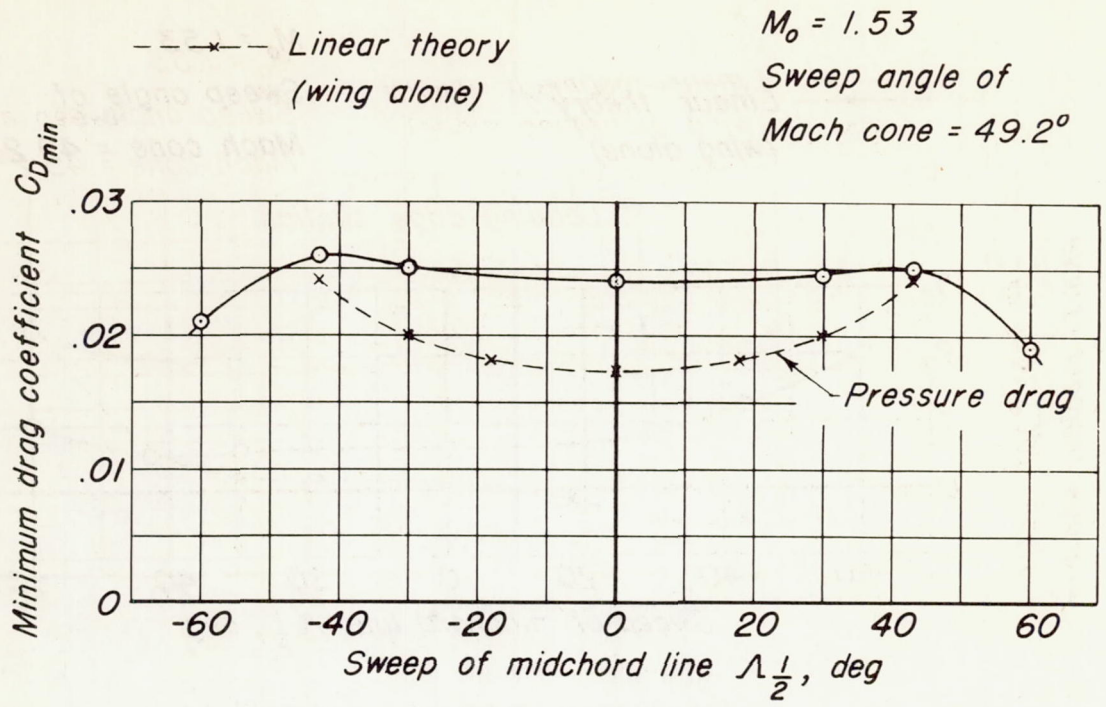

(a) Minimum drag coefficient.

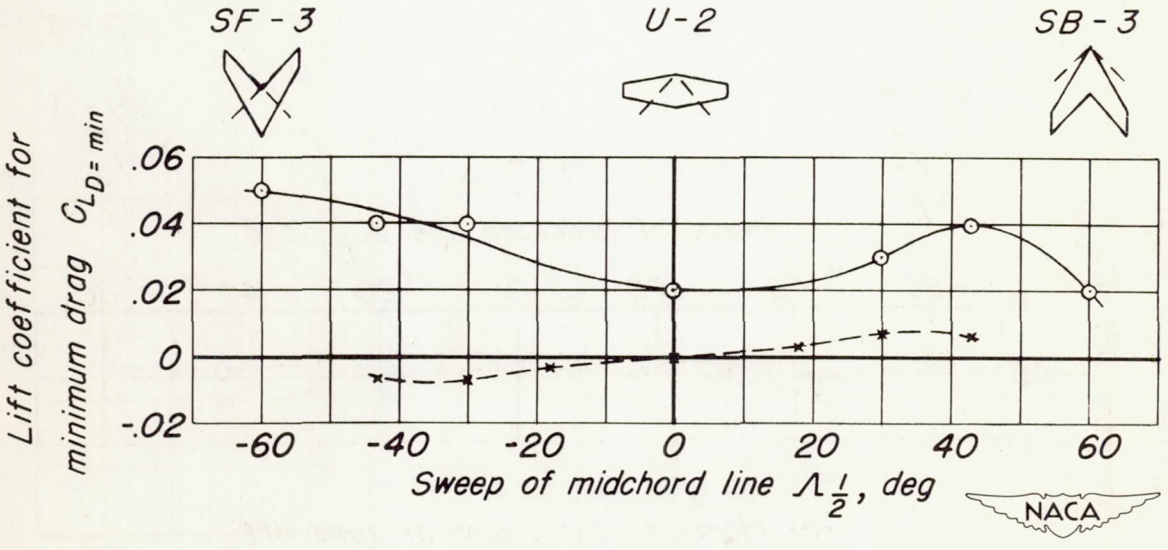

(b) Lift coefficient for minimum drag.

Figure 7. - Minimum-drag charateristics of swept wings.

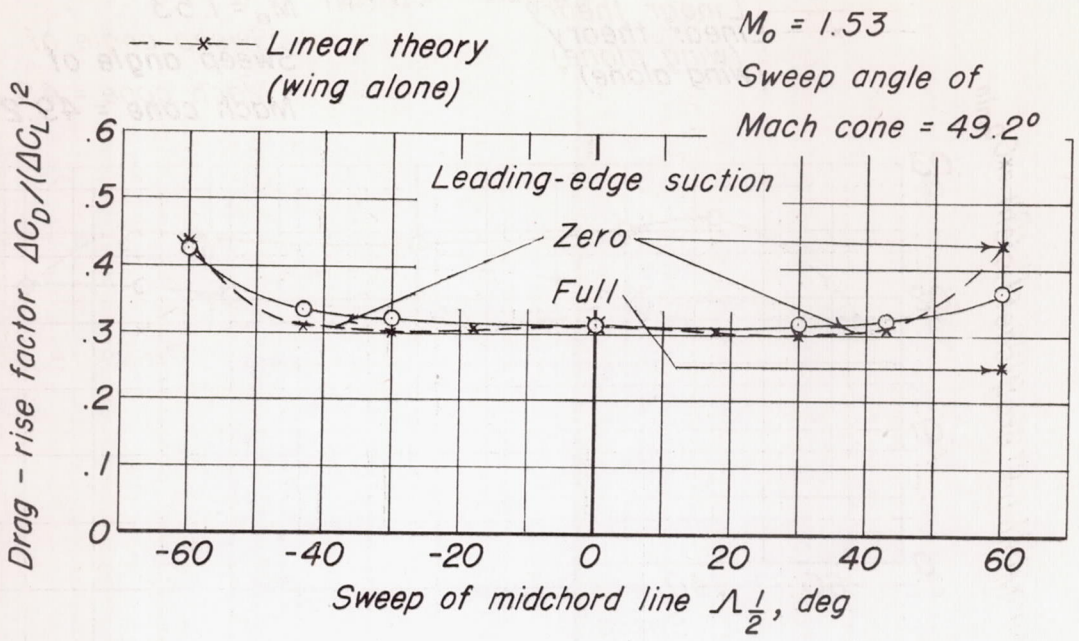

(a) Drag - rise factor.

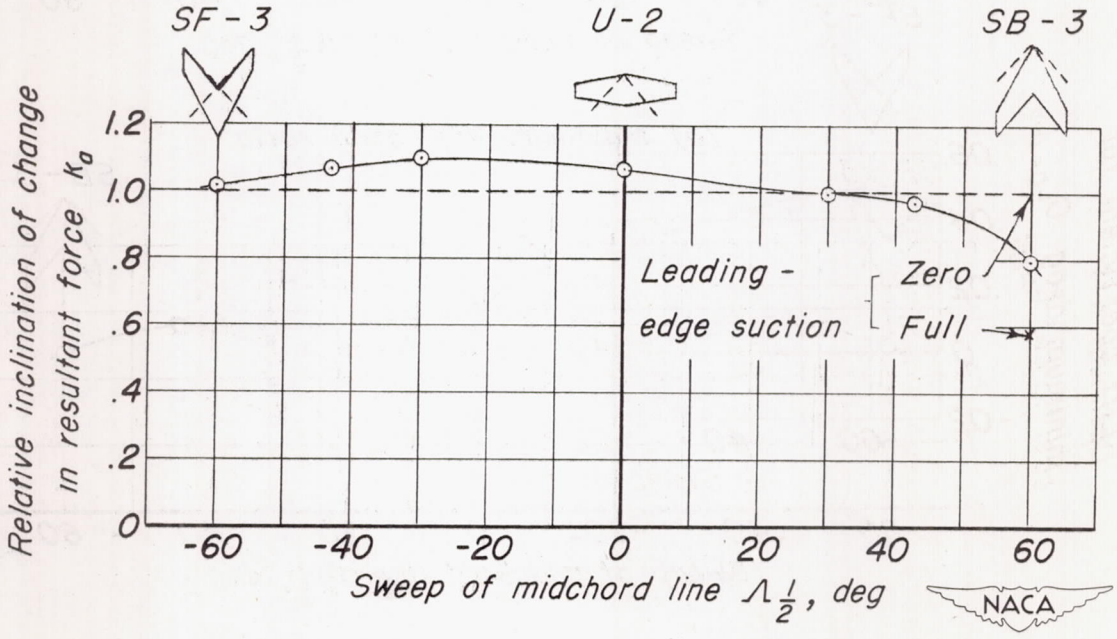

(b) Relative inclination of change in resultant force.

Figure 8. - Drag - rise characteristics of swept wings.

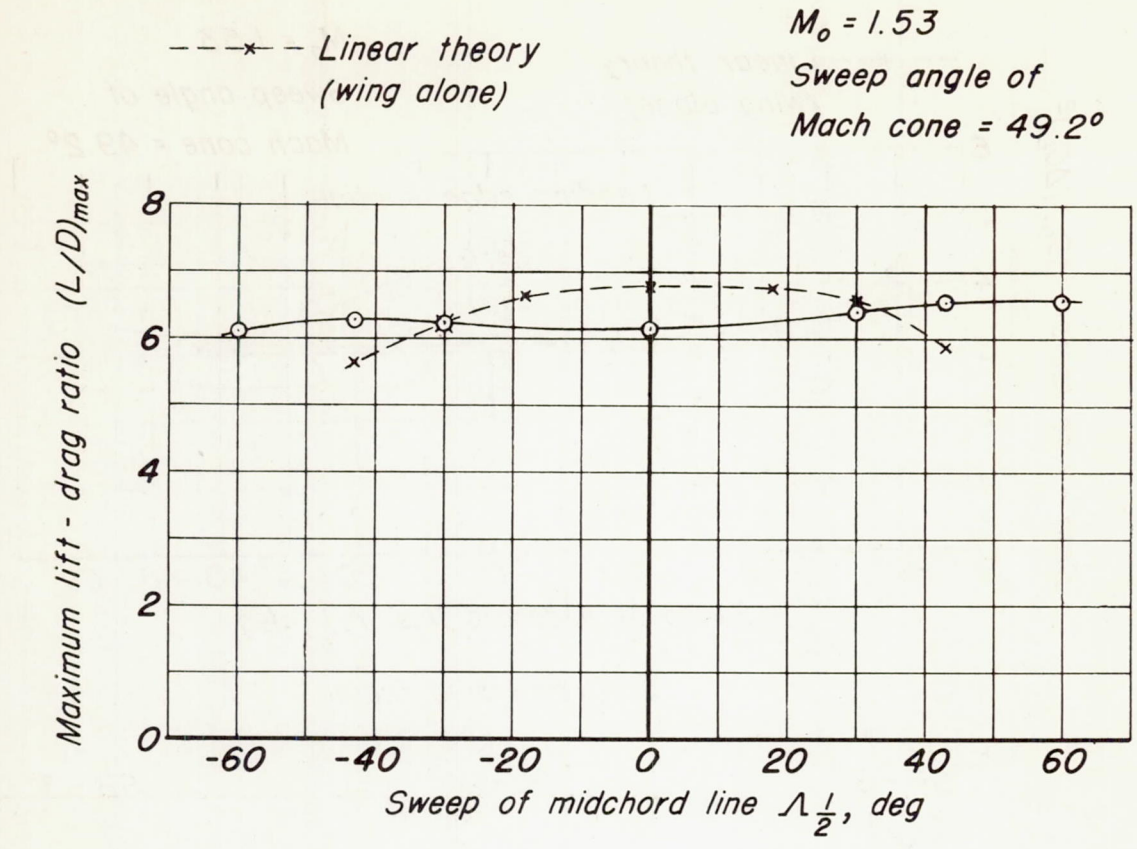

(a) Maximum lift - drag ratio.

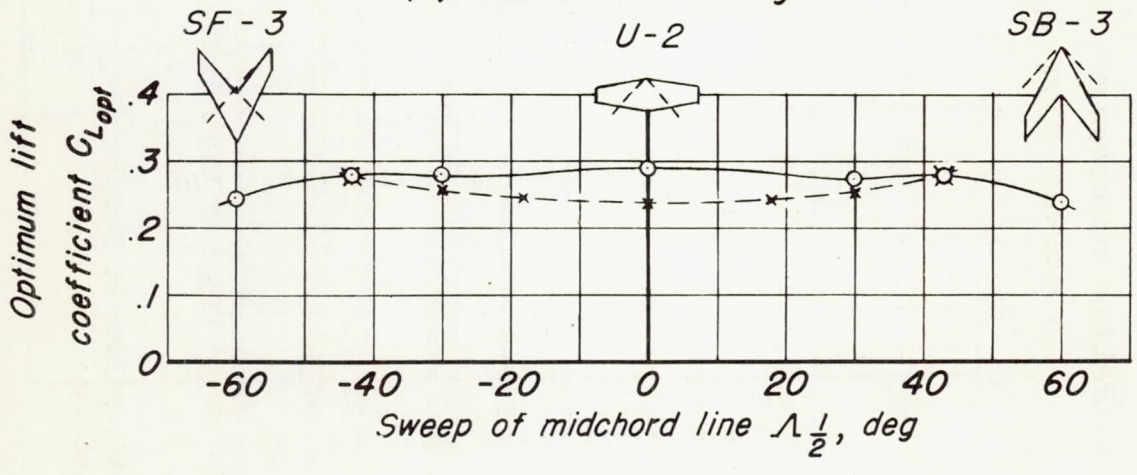

(b) Optimum lift coefficient.

Figure 9. - Maximum lift - drag ratio characteristics of swept wings.